



HAL
open science

Tectono-climatic and depositional environmental controls on the Neolithic habitation sites, Vaigai River Basin, Southern India

Mu U Ramkumar, R. Nagarajan, K J Juni, A. Manobalaji, K. Balasubramani, Priyadarsi D Roy, K. Kumaraswamy, A L Fathima, Athira Pramod, R. Sharveen, et al.

► **To cite this version:**

Mu U Ramkumar, R. Nagarajan, K J Juni, A. Manobalaji, K. Balasubramani, et al.. Tectono-climatic and depositional environmental controls on the Neolithic habitation sites, Vaigai River Basin, Southern India. *Geological Journal*, 2024, 59 (4), pp.1199 - 1218. 10.1002/gj.4919 . hal-04855949

HAL Id: hal-04855949

<https://hal.science/hal-04855949v1>

Submitted on 26 Dec 2024








HAL is a multi-disciplinary open access archive for the deposit and dissemination of scientific research documents, whether they are published or not. The documents may come from teaching and research institutions in France or abroad, or from public or private research centers.

L'archive ouverte pluridisciplinaire **HAL**, est destinée au dépôt et à la diffusion de documents scientifiques de niveau recherche, publiés ou non, émanant des établissements d'enseignement et de recherche français ou étrangers, des laboratoires publics ou privés.

RESEARCH ARTICLE

WILEY

Tectono-climatic and depositional environmental controls on the Neolithic habitation sites, Vaigai River Basin, Southern India

Mu. Ramkumar¹  | R. Nagarajan^{2,3}  | K. J. Juni¹  | A. Manobalaji² |
 K. Balasubramani⁴  | Priyadarsi D. Roy⁵  | K. Kumaraswamy⁶ | A. L. Fathima¹ |
 Athira Pramod¹ | R. Sharveen² | S. Abdul Rahman⁶  | N. A. Siddiqui⁷  |
 D. Menier⁸ | Rajveer Sharma⁹

¹Department of Geology, Periyar University, Salem, India

²Department of Applied Sciences (Applied Geology), Faculty of Engineering and Science, Curtin University Malaysia, Miri, Malaysia

³Curtin Malaysia Research Institute, Curtin University Malaysia, Miri, Malaysia

⁴Department of Geography, Central University of Tamil Nadu, Thiruvavur, India

⁵Instituto de Geología, Universidad Nacional Autónoma de México, Ciudad Universitaria, Coyoacán Ciudad de México, Mexico

⁶Department of Geography, Bharathidasan University, Tiruchirappalli, India

⁷Department of Geosciences, Universiti Teknologi PETRONAS, Seri Iskandar, Malaysia

⁸Geo-Ocean, Univ Bretagne Sud, Univ Brest, CNRS, Ifremer, UMR6538, Université de Bretagne Sud, Vannes, France

⁹Inter-University Accelerator Centre, New Delhi, India

Correspondence

K. J. Juni, Department of Geology, Periyar University, Salem, India.

Email: junikj123@gmail.com

Funding information

Ministry of Earth Science (MoES)

Handling Editor: Y. Anil Kumar

The establishment, development and abandonment and/or destruction of ancient civilizations were catalytically controlled by geomorphic features such as lakes and rivers and the climate. This paper examined the possible influence of tectonism and climate on six habitations of the ancient Vaigai River Basin civilization in South India, using multiple proxies such as grain size, geochronology and geochemistry of the sedimentary archives. The tectonic setting of the basin changed between the active margin and passive margin; the discriminant diagrams suggested varying provenance and changing climatic conditions over the mid- and late Holocene. Tectonic activism and quiescence, base-level change in the channel morphology led to the burial/marooning of the first habitation surface. Overall, arid conditions were punctuated with catastrophic flooding and peak discharge (flood) destroyed the second, third and fourth habitation sites. These flooding events were characterized by moderate weathering (CIA) and high values of Al, Fe and Rb/Sr and low Ca/Mg in the sediment records. The abandonment/destruction of the fifth habitation also occurred during an arid interval (droughts), possibly caused by weak monsoon. Along with the interactions between tectono-climatic and fluvial geomorphic factors, the new results provided avenues to (a) check and recognize the archives for 8.2 and 4.2 ka-like events in this part of the world, and (b) the utility of integrated analyses to constrain on the civilizational histories of the mankind.

KEYWORDS

climatic reversal, geoarchaeological site, geochemical characterization, Vaigai civilization

1 | INTRODUCTION

The stories about the adoption of early as well as present-day human life to environmental conditions provide information on the strategies adopted and their efficacy in survival or decimation (Li et al., 2013; Redman et al., 2004). Settlements along the active rivers and coasts were provided with crucial resources such as water and fertile

floodplain for agriculture (Huitema & Meijerink, 2017). The climate and its cause-effect responses to the fluvial system have played significant roles in sustaining and destructing the habitation sites. For example, the intervals of higher humidity and more stable summer precipitations were considered propitious to agriculture in southern Mesopotamia (Kennett & Kennett, 2007). The expansion of agriculture in the Indus Basin between 10,000 and 7000 cal. years BP occurred during an

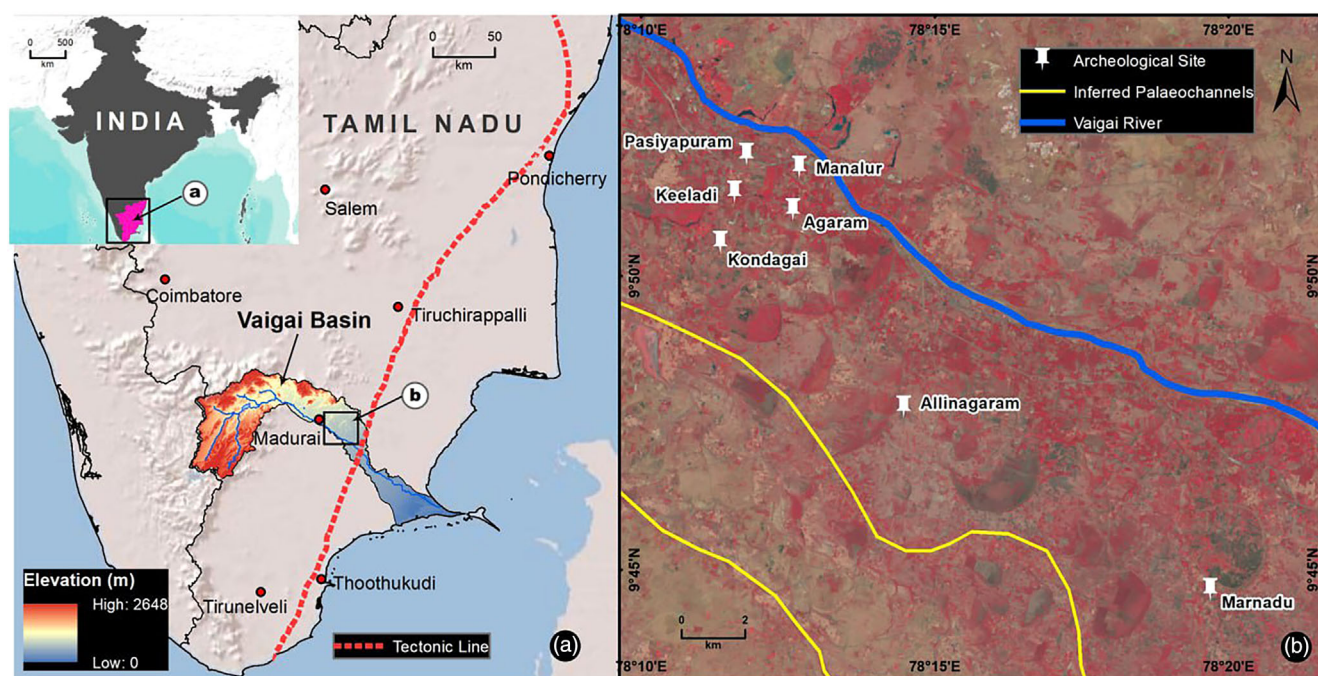


FIGURE 1 Location of the Vaigai River Basin. The inset shows the regional tectonic line that delimits the delta head in all the major river systems of southern India including the Vaigai River. Ramkumar et al. (2016) demonstrated its genesis during Precambrian and continued activism until recently. The palaeochannel courses recognized in the vicinity of the present-day Vaigai River channel recognized through remote sensing, digital image processing and field mapping (see for details Ramkumar et al., 2021; Ramkumar, Balasubramani, et al., 2022) and the locations of geoarchaeological excavations and sampling are also indicated in this figure.

interval of suitable climate (Gupta, 2004). The changes in land-forming processes, especially through the catastrophic floods, caused by tectonics along with climate, have also played a major role in the demise/burial of ancient civilization sites (Field et al., 2007; Ramkumar et al., 2019). The unforeseen responses of bed elevation to climate change have important implications for the survival-demise/burial along the river banks (Slater & Singer, 2013; Thakur et al., 2016; Ramkumar et al., 2015, 2021). The Indus civilization was river-based as two of its largest and most well-known cities, Harappa and Mohenjodaro, were situated next to the perennial Himalayan rivers (Possehl, 2002; Singh et al., 2017). The Ghaggar-Hakra system became ephemeral and largely abandoned after about 4000 cal. year BP is one of the examples of a climate-controlled landscape (Giosan et al., 2012). The Nile River civilization (2400–1300 B.C.) managed recurrent catastrophic floods by using the newer floodplains for agriculture (Macklin et al., 2013). However, a few catastrophic events have also caused the abandonment of ancient habitation sites. The prevalence of long-term droughts during the early to middle Holocene was contemporary with the collapse of many civilizations (Mehrotra et al., 2019). The demises of major civilizations across the globe have been clubbed into the 8.2 and 4.2 ka events (for example, Bar-Matthews & Ayalon, 2011; de Menocal, 2001; Madella & Fuller, 2006; McIntosh, 2007; Perry & Hsu, 2000; Possehl, 2002; Ristvet & Weiss, 2005; Stanley et al., 2003; Staubwasser et al., 2003; Staubwasser & Weiss, 2006; Weiss, 2000; Weiss et al., 1993; Weninger et al., 2006).

Some of the religious-cultural sites buried under the flood deposits of the Cauvery River and at the apex of the Vaigai River delta

were recently unearthed (Ramkumar et al., 2018, 2021). These east-flowing, major river systems of southern India have also evidence of ancient (Micro-Neolithic) habitation sites marooned under the historic-prehistoric flood deposits (Figure 1). Previous studies surmised that the lack of awareness about cyclic and/or episodic flooding in the river and associated flood control measures might have led to the burial and abandonment of the habitation sites in these river systems (e.g. Ramkumar et al., 2021; Ramkumar, Balasubramani, et al., 2022). The hypothesis about the causal link between climate and civilization sites in southern India, along the three major river systems, has necessitated the examination of the establishment-abandonment dynamics and spatial-temporal scales of variations in tectonics, climate and depositional environmental setting.

2 | REGIONAL SETTING

The Vaigai River Basin covers an area of 7380 km² covering the Theni, Madurai, Dindigul, Sivagangai and Ramanthapuram districts of Tamil Nadu State in India (Juni et al., 2022; Figure 1). It has a tropical climate with rainfall (average 800 mm/year) during both the Southwest (June–September) and Northeast (October–December) monsoons. There is a marked disparity of annual rainfall across the basin with 1270 mm at the western extremity and 635 mm at the eastern extremity (<http://indiawris.gov.in/wiki/doku.php?id=vaigai>). The river originates at Varusanadu hills of the Western Ghats range and debauches into the Bay of Bengal through a brackish lake after and flowing for about 270 km. The

basin morphology was probably caused by techno-morphological events (Juni et al., 2022; Ramkumar et al., 2019). The tectonic evolution led to a continental arc above a subduction zone and the Karur-Kambam-Painavu-Trichur shear zone (KKPT) divided the Archean and Proterozoic rocks in this basin (Ghosh et al., 2004).

Geologically, the northern part of the basin is represented by Neoproterozoic/Palaeoproterozoic felsic rocks and intermediate charnockite with metasedimentary rocks such as quartzites, calc-silicates and high- to ultrahigh-temperature metapelites (Chetty, 2021; Drury et al., 1984; Rajesh & Santosh, 2012; Sajeev et al., 2006). Charnockite (Neoproterozoic) with metasedimentary rocks such as Mg, Al granulites, garnet-biotite-sillimanite gneiss, garnet-biotite gneiss, quartzites and calc-silicates constitute the southern part of the basin (Chetty, 2021; Gao et al., 2021; Santosh et al., 2009; Santosh et al., 2017). Over this terrain, Ramkumar et al. (2018) documented tectonically quiescent regions and multiple incisions by the river channels during the five different landscape development stages and they were evidenced by spatial variability of morphometric measurements (Juni et al., 2022). The stages are represented by the inheritance of river basins from palaeodrainage systems, reversal of river flow directions during the early Cenozoic and inception of the modern river

systems, during the Miocene–Pliocene, Pleistocene, early Holocene and the Holocene–Anthropocene (Ramkumar et al., 2018).

3 | METHODS AND MATERIALS

The present study involves facies characterisation, interpretation of depositional and erosional episodes based on field observations and the mineralogical and geochemical analyses of selected sediments for the interpretation of palaeoclimate, tectonic setting, provenance, etc. These were followed by the integration with geochronological constrain of the relative influences of tectonic, climatic and depositional environments on the establishment, survival and abandonment/destruction of habitation sites.

The archaeological excavations at Keezhadi and Agaram were chosen for sediment sampling as per Ramkumar et al. (2021). A total of 62 sediment samples were collected from three pits (5 from Keezhadi pit-1, 30 from Keezhadi pit-2 and 27 from Agaram pit). Approximately 1 kg of each sample was collected and packed in airtight PVC bags, labelled and transported to the laboratory. The field logging of facies, sedimentary structural and archaeological information and photologs were used to create the lithologs (Figure 2a,b).

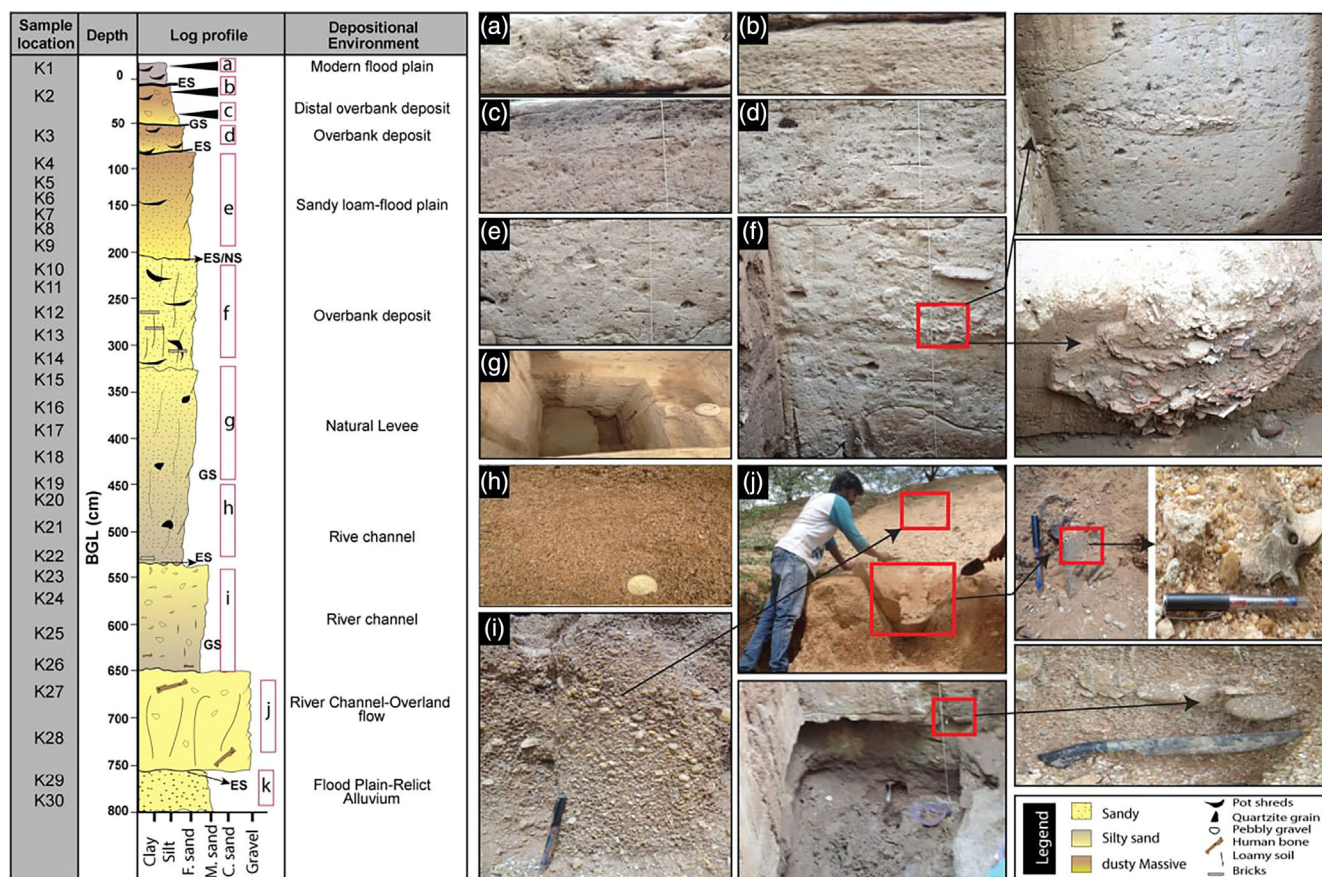


FIGURE 2 Photolog and lithology of the (2a) Keezhadi, (2b) Agaram (modified after Ramkumar et al., 2021; Ramkumar, Balasubramani, et al., 2022). Lithologs, facies characteristics, interpreted depositional environments based on facies and granulometry, stratigraphic locations of artefacts and numerical ages of the studied sections are shown.

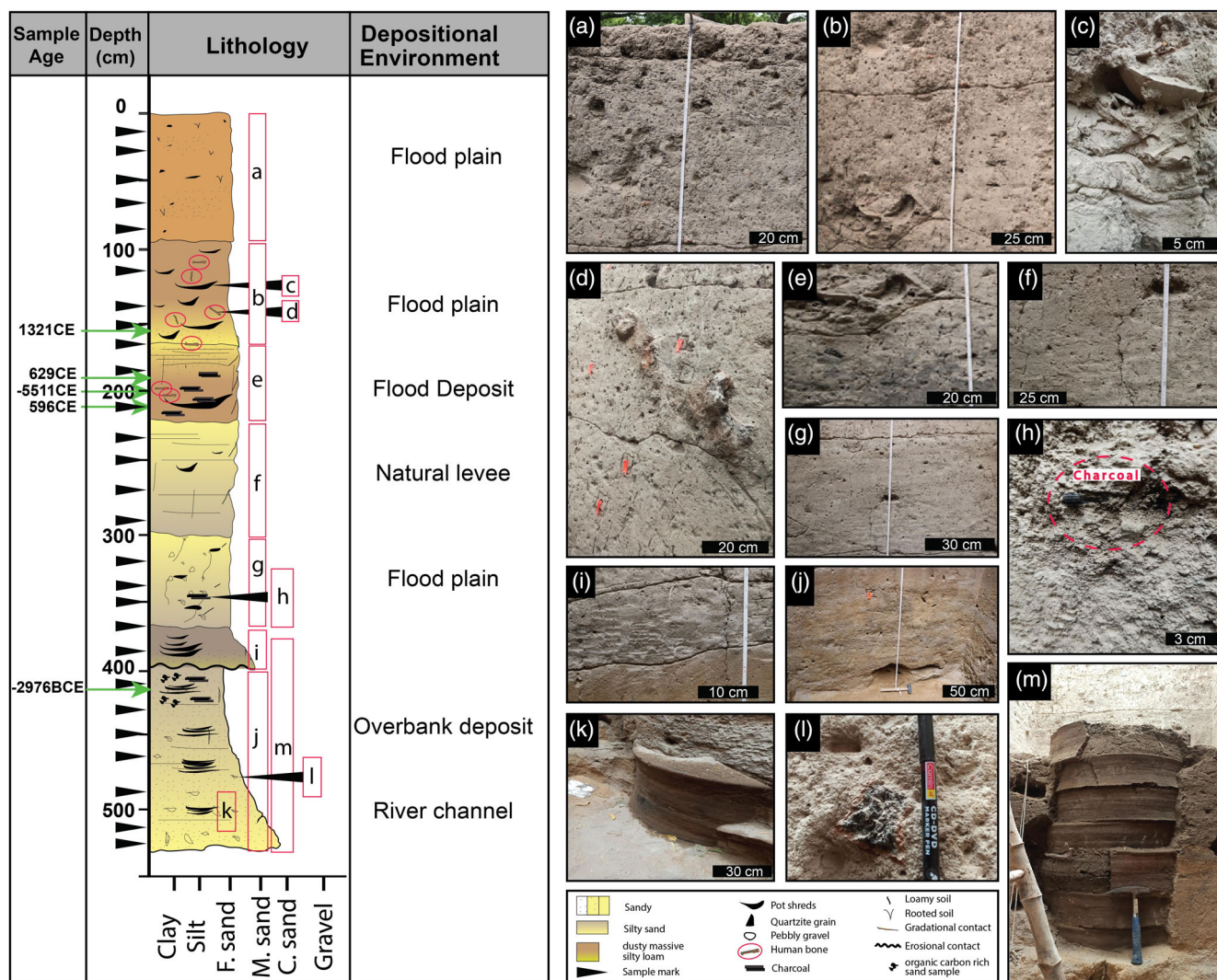


FIGURE 2 (Continued)

3.1 | Granulometry

All the sediment samples collected (62 Nos.) were subjected to size analysis following Folk and Ward (1957). About 150–200 g of each sample was air-dried and the visibly recognizable shell fragments, organic material and pebbles were removed. A sub-sample of about 30–40 g, through coning and quartering, was processed by adding H_2O_2 and HCl to remove organic matter and shell material. Samples were subsequently treated with HNO_3 and quasi-distilled water and again dried overnight at $60^\circ C$. They were weighed and dry-sieved in an automated sieve-shaker with ASTM test sieve sets of $\frac{1}{2} \phi$ intervals (Ingram, 1970) as per Ramkumar et al. (2000) and Ramkumar (2001, 2007). The cumulative percent in ϕ intervals were plotted in a semi-log graph sheet to compute the graphic mean (Mz), standard deviation (SD), skewness (SK) and kurtosis (KG) and to elaborate a few bivariate plots.

3.2 | Geochemistry

Dry ($\sim 60^\circ C$) and homogenized sediment samples of the Keezhadi pit (Figure 2a) were pulverized to $< 63 \mu m$ using an agate mortar and pestle for the estimation of major oxides in X-Ray Fluorescence (XRF) spectrometer after quantifying the loss on ignition (LOI). Trace elements were measured in an inductively coupled plasma mass spectrometry (ICP-MS) after digesting in an aqueous media. Total carbon and sulphur were determined by the Leco method (TC003). The accuracy was better than 5% for major oxides and better than 10%–11% for trace elements. Blank replicate and standard (SO-19) analyses were performed to ensure the accuracy of the analysis.

The geochemical data were used for chemostratigraphy and interpretation of tectonic setting, provenance, weathering trend and climate. The intensity of weathering of siliciclastic fractions in sediments was estimated by calculating the chemical index of alteration (CIA) as per Nesbitt and Young (1982) and plagioclase index of alteration (PIA)

as per Fedo et al. (1995). CaO in the siliciclastic fraction was estimated using the methods of McLennan et al. (1993), Bock et al. (1998), Nagarajan et al. (2017) and Overarea et al. (2021). CaO was used for further calculation when it is less or equal to Na₂O. It was replaced with Na₂O values in samples where CaO is higher than Na₂O.

3.3 | Mineralogy

A total of 30 samples from the Keezhadi pit were powdered using an agate mortar and pestle to <63 µm size and the powders were analysed for mineralogy through X-Ray Diffraction. The analyses were performed in Physics laboratory, Periyar University. The samples were measured at 2 theta (θ) angles between 3° and 80° continuously with a step size of 0.01° following the standardized protocol. The resultant diffractograms were examined with the help of HighScore Software manufactured and licensed by Panalytical B.V., for peaks, patterns and phases to identify mineral species present in the samples.

3.4 | Geochronology

A total of 25 samples were initially chosen for ¹⁴C dating at IUAC (Inter-University Accelerator Centre), New Delhi (Sharma et al., 2019), and only 15 samples qualified for the age determination due to availability of measurable carbon contents. They were pretreated using the ABA (Acid-Base-Acid) protocol and graphitized using Automated Graphitization Equipment (AGE). ¹⁴C/¹²C ratios in the graphite were measured using XCAMS (the compact ¹⁴C accelerator mass spectrometer extended for ¹⁰Be and ²⁶Al) and converted into radiocarbon ages using the method described in Stuiver and Polach (1977). All the

radiocarbon ages (BP) were calibrated to the calendar years (BCE/CE) using OxCal (v 4.4.4) software and Bayesian age-depth modelling (Bronk Ramsey, 2009). In addition, chronological timelines from previous publications were also referred in this study (Ramkumar et al., 2019, 2021; Ramkumar, Balasubramani, et al., 2022).

4 | RESULTS

4.1 | Chronology

All these chronological data from the present study and compiled from previous publications (Table 1) with respect to archaeological habitation surfaces are presented in Figure 3.

4.1.1 | Keezhadi Pit

In pit-1, the organic matter preserved in sediments at 325 cm depth represented 5359–4942 BCE, at 270 cm represented 3346–2589 BCE and at 160 cm represented 1211–997 BCE. In pit-2, the organic carbon in sediments at 250 cm depth represented 752–406 BCE and this sample is relatively far from the present-day channel course.

4.1.2 | Agaram Pit

All the radiocarbon ages are stratigraphically consistent, except for one bone clast. The bone clast recovered at 170 cm depth yielded the youngest (1278–1390 CE) radiocarbon age of this sequence.

TABLE 1 Radiocarbon age of selected samples and their stratigraphic positions (Source: Ramkumar et al., 2019, 2021; Ramkumar, Balasubramani, et al., 2022).

S.No.	Sample name	Depth (cm) below surface	Calibrated ages (BCE/CE)
1	Bone ^a	170	1278 CE – 1390 CE
2	Organic Carbon ^b	45	1167 CE – 1269 CE
3	Charcoal ^a	198	599 CE – 659 CE
4	Charcoal ^a	216	555 CE – 644 CE
5	Sediment ^c	230	412 BCE – 237 BCE
6	Sediment ^c	250	752 BCE – 406 BCE
7	Sediment ^a	160	1211 BCE – 997 BCE
8	Sediment ^a	240	1613 BCE – 1414 BCE
9	Sediment ^a	205	2136 BCE – 1620 BCE
10	Sediment ^a	270	3346 BCE – 2589 BCE
11	Sediment ^a	430	3307 BCE – 2878 BCE
12	Sediment ^a	325	5359 BCE – 4942 BCE
13	Charred Bone clast ^a	200	5627 BCE – 5370 BCE
14	Human Bone 3 ^c	155	778 CE – 1016 CE
15	Human Bone 2 ^c	135	689 CE – 883 CE

^aData from Ramkumar, Balasubramani, et al. (2022).

^bData from Ramkumar et al. (2019).

^cData from Ramkumar et al. (2021).

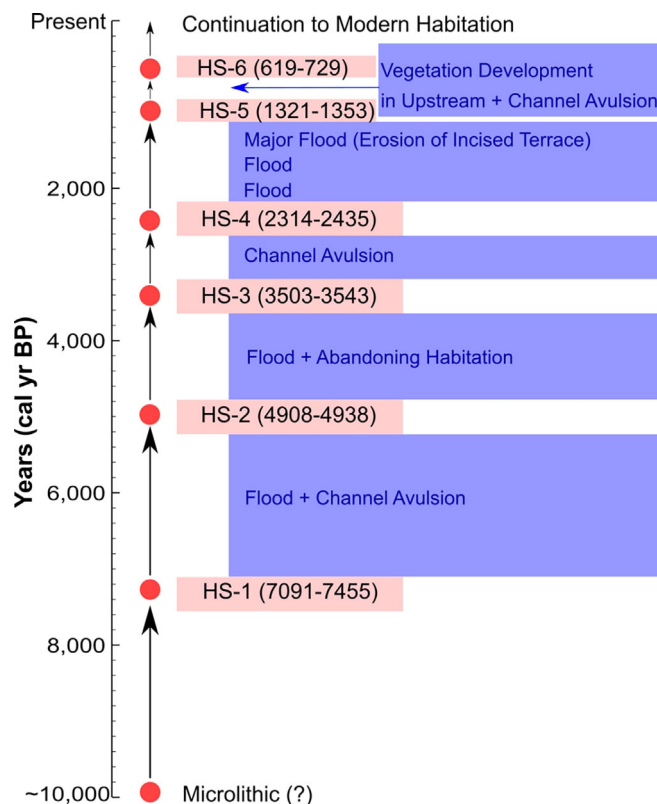


FIGURE 3 Chronology of habitations interspersed with channel avulsion and flooding events (modified after Ramkumar, Balasubramani, et al., 2022). The figure demonstrates the recurrent relative roles of regional landscape evolution, cyclic and extreme climatic events. Their causal relationship with the establishment, shifting, evolution, survival, abandonment and or reestablishment events of habitational sites could also be discerned.

The charcoals at depths of 216 and 198 cm yielded comparable ages of 555–644 CE and 599–659 CE, and both were collected from a layer of flood deposits. Bulk organic carbon constrains the sediment at 430 cm depth to 3307–2878 BCE. The charred bone clast at 200 cm with the oldest age (5627–5370 BCE) of this sequence was recovered from the layer of flood deposit constrained between 555 and 644 CE and 599–659 CE indicating its reworked nature. The youngest age estimate of 689–883 CE is obtained at Agaram, a location situated nearest to the present-day channel course. The bone fragments were dated to be 778–1016 CE and 689–883 CE.

4.2 | Textural and facies characteristics

4.2.1 | Keezhadi pit

Most of the sediments of pit-1 were very poorly sorted with finely skewed at the bottom and are very finely skewed up to the top except for the symmetrical nature of one sample below the topmost layer

(Figure 2a). They were mesokurtic in the bottom and leptokurtic up to the top. In pit-2, most of the samples were fine sand, and a few samples in the bottom were coarse to medium and interspersed with very fine sand towards the middle part. Only two samples showed moderate sorting and the remaining are poorly sorted. The bottom samples were fine-skewed and the top is near symmetric. Most of the samples were platykurtic, mesokurtic in the bottom with an interlayer of sediments with leptokurtic character.

4.2.2 | Agaram pit

Sediments were mainly fine sand, interspersed with very fine sand towards the lower part and interlayers of medium sand and coarse sand at the top. Textural parameters such as mean size (Mz), standard deviation (SD), skewness (SK) and kurtosis (KG) were monotonous at the bottom and changed to high-frequency variations in the middle and showed extreme variability at the top. Except for three samples with moderate sorting, all the samples were poorly sorted. The skewness showed a range from fine-skewed to very coarse-skewed. Most of the samples were leptokurtic to extremely leptokurtic. Sediments representing the erosional surfaces and intense human-habitation surfaces were coarse- and very coarse-skewed. A gradual fining-upward nature superimposed on episodic changes in these textural characteristics forms an overall long-term linear trend of fining, a shift from moderate to poor sorting, a change from very coarse-skewed to symmetric fine-skewed and a change from mesokurtic to very leptokurtic. Stratigraphic variations of the textural information are presented in Figure 4. The discriminant plots of sediment character, depositional energy, depositional environment and transport modes are presented in Figure 5a–e.

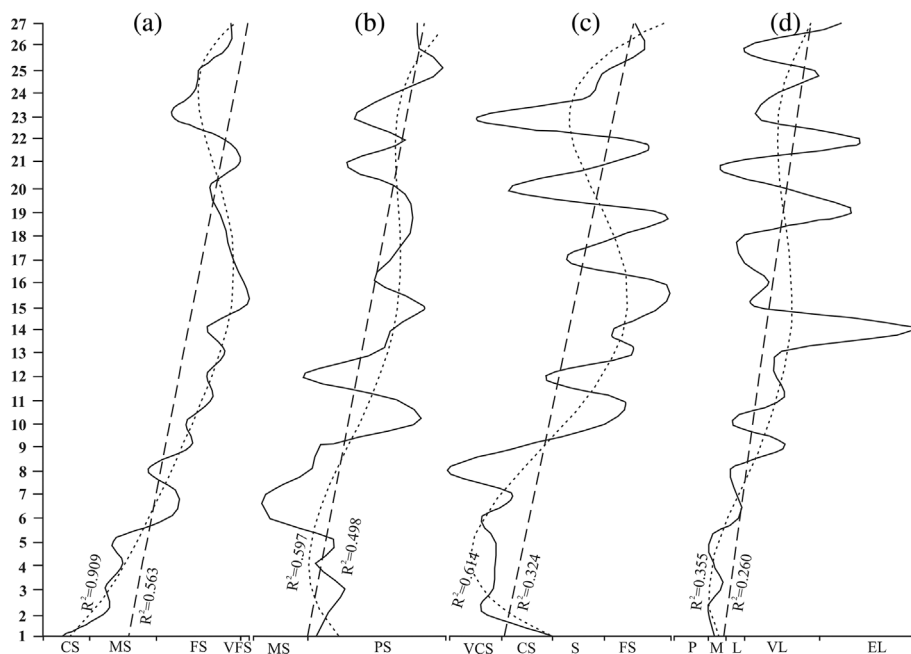
4.3 | Mineralogy

The bulk mineralogy of the Keezhadi pit samples is summarized in Table S1. The Keezhadi pit sediments mainly consist of quartz, feldspar, pyroxene, beryl group of minerals, Ti-oxide minerals, mica and arsenates and other minerals such as feldspathoid, zeolite, amphibole and sulphide group are recorded in selective samples. Samples are rich in amorphous materials; however, the total amorphous minerals were not quantified in the present study. Also, secondary minerals of sulphides and oxides were recorded in many samples. The arsenates are mainly Cs and Sc bearing and arsenolite was also recorded.

4.4 | Geochemistry

Geochemical profiles (Figure 6) revealed the stratigraphic variations in abundances of illite, kaolinite and smectite. Higher Na/Al values indicated the presence of more smectite in the upper sediments while low Na/Al in the bottom samples showed less smectite. The Ga/Rb

FIGURE 4 Stratigraphic variations of the textural parameters, Agaram section. (a) mean size; (b) standard deviation; (c) skewness; (d) kurtosis. The solid line shows the absolute values, the dashed line shows the linear trend and the dotted line shows the polynomial trend. Short-term changes in the absolute values of all the parameters, a gradual shift of coarse to fine grain size (Mz), moderate to poor sorting (SD), very coarse-skewed to fine-skewed (SK) and mesokurtic to leptokurtic (KG) nature in linear trend and a double cyclic nature in polynomial trend are discernible. Together they indicate natural geological environmental variability, anthropogenic interference, resultant mixing of sediments, etc.



ratio of the bottom samples can be connected to the high kaolinite. Ratios of Rb/Al, K/Al and K/Rb, indicated the presence of illite, and also its higher proportion in the bottom samples. The chemostratigraphic profiles of CIA, Fe, Al and Ca/Mg and Rb/Sr ratios also corroborate with these trends (Figure 7). CIA profiles indicated a range from low to moderate weathering, with the bottommost samples (K30-K29). The next set of samples (K28-K27) demonstrated lower weathering and the subsequent set of samples (K26-K25) exhibited increasing CIA values. Samples K25, K24, K23 and K22 showed a trend of gradually decreasing CIA values from moderate to low weathering. The profiles of CIA, Fe, Al and Rb/Sr indicated progressive changes from sample K30 to K16 and generally homogeneous trends for sample K16 to K1 except for the Ca/Mg profile. Based on the $\log(\text{SiO}_2/\text{Al}_2\text{O}_3)$ vs. $\log(\text{Fe}_2\text{O}_3^*/\text{K}_2\text{O})$ plot of Herron (1988), most samples are classified as wacke ($n = 18$) followed by litharenite ($n = 6$) and shale ($n = 6$) (Figure 8).

4.4.1 | Major oxides

SiO_2 showed more highest variation (37.31–81.82 Wt.%) in litharenite compared with wacke (65.64–72.31 Wt.%) and shale (60.91–64.41 Wt.%). Average values of SiO_2 also remained higher in litharenite (avg. 68.92 Wt.%) than in wacke (avg. 68.29 Wt.%) and shale (avg. 62.33 Wt.%). Al_2O_3 in shale (14.35–17.35 Wt.%, avg.16.22 Wt.%) was higher than litharenite (4.11–11.18 Wt.%, avg.8.59 Wt.%) and wacke (11.44–14.73 Wt.%, avg.12.79 Wt.%). Al_2O_3 contents were higher in samples K26–K24, K19 and lesser in K7. Fe_2O_3 in shale (7.06–12.10 Wt.%, avg. 8.72 Wt.%) was higher than litharenite (2.36–6.99 Wt.%, avg.4.41 Wt.%) and wacke (4.42–6.80 Wt.%, avg.5.94 Wt.%). K_2O , Na_2O , P_2O_5 in shale (3.03–3.54 Wt.%, avg.3.37 Wt.%), (1.87–2.29 Wt.%, avg.2.08 Wt.%), (0.19–1.02 Wt.%, avg.0.50 Wt.%) and

litharenite (0.93–3.36 Wt.%, avg.2.34 Wt.%), (0.44–2.07 Wt.%, avg.1.24 Wt.%), (0.05–1.67 Wt.%, avg.0.58 Wt.%) were less compared with wacke (2.75–3.63 Wt.%, avg.3.14 Wt.%), (1.40–2.50 Wt.%, avg.1.83 Wt.%), (0.193–2.07 Wt.%, avg.1.22 Wt.%). TiO_2 was also recorded higher in shale (0.86–2.52 Wt.%, avg.1.23 Wt.%) than wacke (0.65–1.09 Wt.%, avg.0.79 Wt.%) and litharenite (0.34–1.33 Wt.%, avg. 0.69 Wt.%). CaO showed lower abundance in wacke (2.70–5.95 Wt.%, avg.4.11 Wt.%) and shale (2.29–4.48 Wt.%, avg.3.41 Wt.%) and higher abundance in litharenite (2.07–52.54 Wt.%, avg.11.72 Wt.%).

4.4.2 | Trace elements

Rb content in all the samples was depleted compared with UCC (Figure 5). It was highest in shale (102.95 ppm) than in wacke (89.29 ppm) and litharenite (59.26 ppm). It also showed a strong to moderate positive correlation with Al_2O_3 ($r = 0.938$), K_2O ($r = 0.822$) and Fe_2O_3 ($r = 0.655$), MnO ($r = 0.570$) and MgO ($r = 0.629$). Ba was enriched relative to UCC and it was more in shale (1368.33 ppm) and wacke (1314.83 ppm) compared with litharenite (1000 ppm). It exhibited a strong positive correlation with Na_2O ($r = 0.947$) and K_2O ($r = 0.969$) and a moderate positive correlation with Al_2O_3 ($r = 0.759$). Low Sr in litharenite (336.53) and high Sr in wacke (438.53 ppm) and shale (393.20 ppm) were reflected by weak to moderate correlation with Al_2O_3 ($r = 0.519$), MnO ($r = 0.561$), Na_2O and K_2O ($r = 0.673$, $r = 0.671$, respectively). Cr, Ni, V, Co and Sc (avg.131.13 ppm, 56.33 ppm, 128.66 ppm, 22.65 ppm, 15.66 ppm, respectively) remained higher in shale than wacke (avg. 91.99 ppm, 41.89 ppm, 87.44 ppm, 16.93 ppm and 11.17 ppm, respectively) and litharenite (avg. 64.99 ppm, 26.48 ppm, 75 ppm, 10.76 ppm and 7.83 ppm respectively). All of them in wacke and litharenite were depleted compared with UCC. Cr contents in wacke and shale,

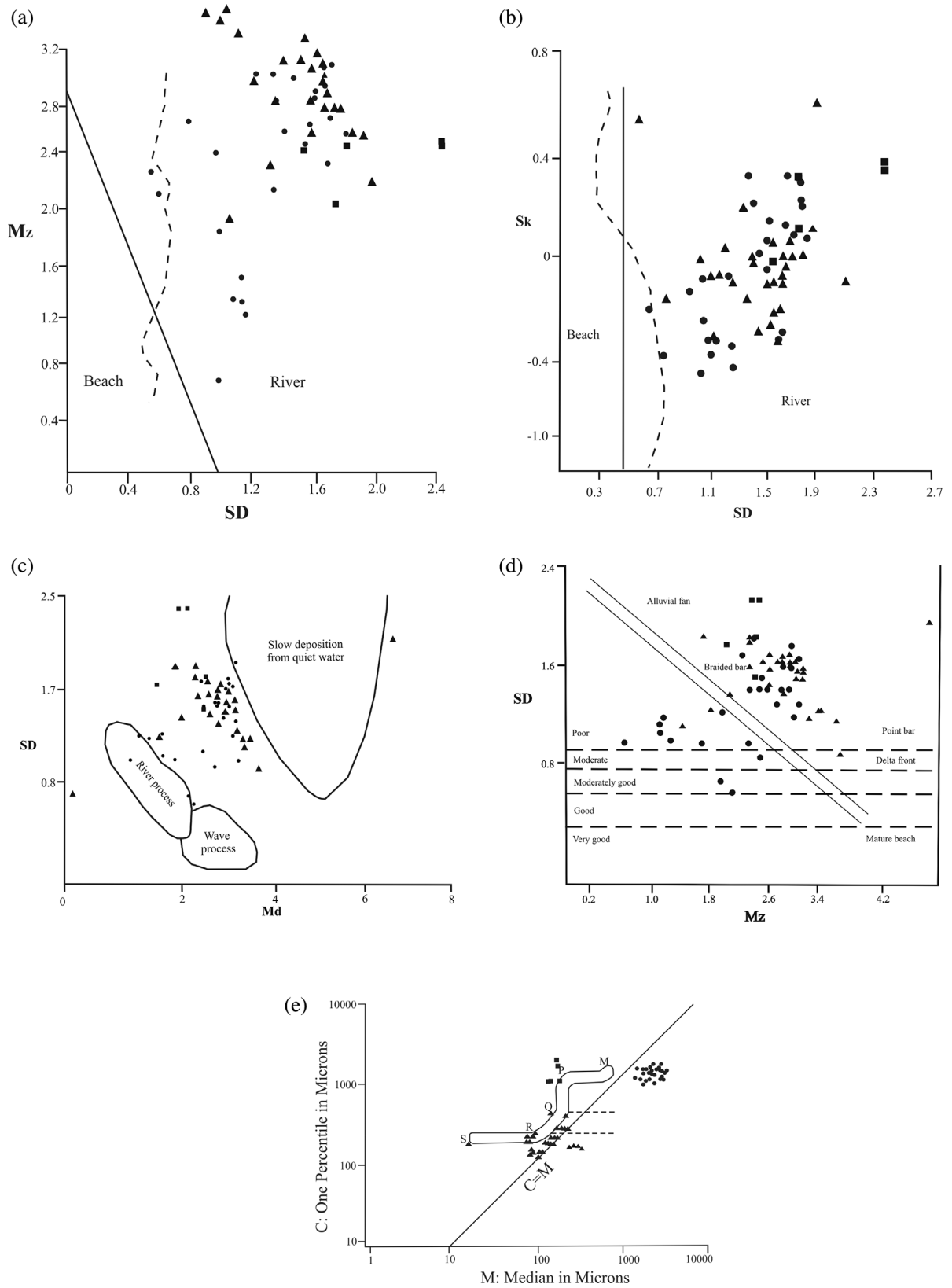


FIGURE 5 Legend on next page.

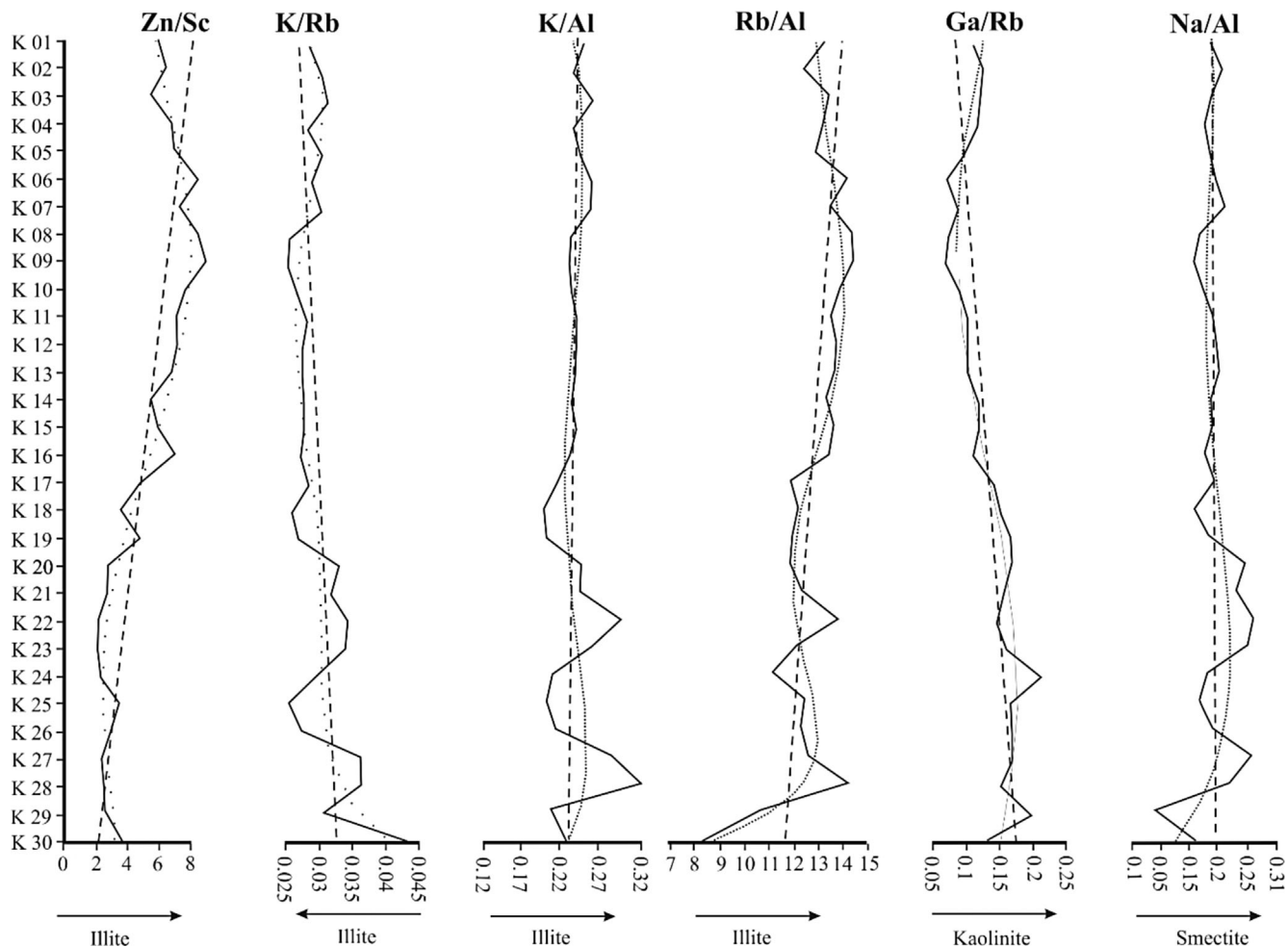


FIGURE 6 Stratigraphical profiles of clay indicators. Collectively the difference between the bottom and upper parts of the studied section is indicated, perhaps due to the climatic and or depositional environmental changes.

however, were enriched compared with UCC. High-field-strength elements (HFSE) such as Y, Zr, Nb, Th and Hf also recorded higher concentrations in shale (26.08 ppm, 532.38 ppm, 15.75 ppm, 20.25 ppm

and 13.26 ppm, respectively) when compared with wacke (18.66 ppm, 386.84 ppm, 10.44 ppm, 14.54 ppm and 9.69 ppm, respectively) and litharenite (12.01 ppm, 302.03 ppm, 8.93 ppm, 12.75 ppm and

FIGURE 5 Interpretation of depositional environment, energy and transport modes. The samples from the Keezhadi pit-1 are shown in triangle, samples from the Keezhadi pit-2 are shown in solid squares and the samples from the Agaram are shown in circle. (a,b) Discriminant diagram of River-Beach environment based on Friedman (1967) and Moiola and Weiser (1968). These diagrams show that all the samples fall in the river field, affirming the deltaic/fluvial setting. However, the extremely scattered nature of the data points, although these are collected from a single regional setting, suggests extreme variations in depositional energy conditions, variable sourcing of sediments in terms of provenance and/or exhumation surfaces in the catchment and depocenters, flow conditions, etc. (c) Discriminant diagram of River-Wave-Quite environments based on Stewart (1958) suggests plot of almost all the samples between river process (unidirectional flow) and stillwater conditions. This observation reinforces the variable conditions of sourcing, deposition and energy conditions interpreted based on a and b. (d) Determination of depositional environment based on Glaister and Nelson (1974) suggestive of plotting of all the samples within the range of alluvial fan to delta front. This observation affirms the interpretation of differential exhumation and other variabilities interpreted based on (a–d). Further, recycling and mixing of fresh as well as older sediments are also indicated as few to many of the samples fall near the alluvial fan field. (e) Determination of modes of sediment transport (after Passega, 1957). The field M-O indicates sediments that are transported by rolling, O-P rolling and suspension, P-Q suspension with rolling, Q-R graded suspension and R-S uniform suspension. The upper dashed horizontal line indicates maximum grain size transported by graded suspension and the lower dashed horizontal line indicates maximum grain size transported by uniform suspension. While the plot of two different clusters in terms of locations of sample collection (Keezhadi and Agaram) may indicate the spatial difference of depositional/transportational and or post-depositional anthropogenic interference factors, the plot below the C = M line suggests affirmatively the anthropogenic interference and or extreme climatic event or both.

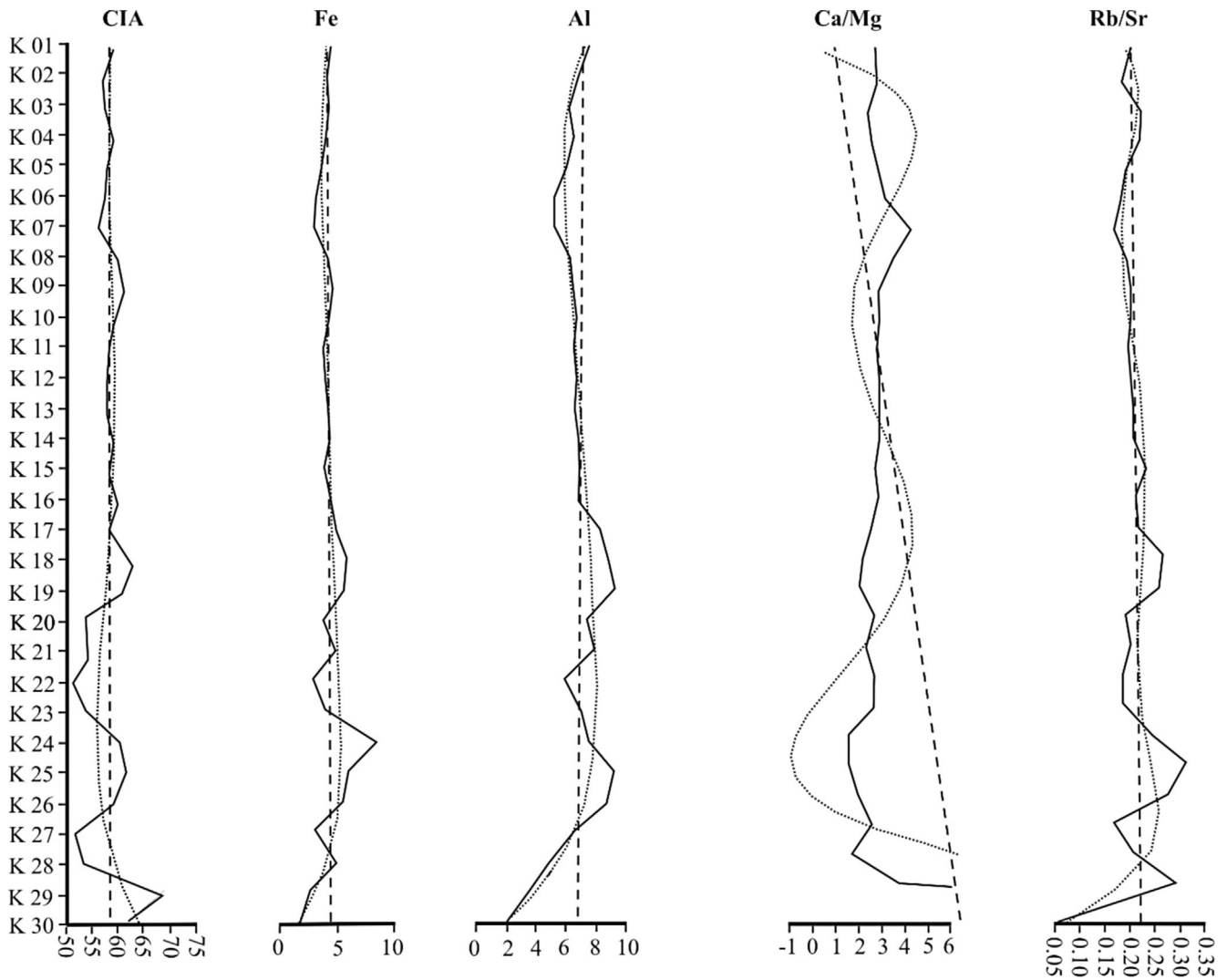


FIGURE 7 Geochemical profiles of CIA, Fe, Al, Ca/Mg and Rb/Sr value. Regional stability of the climate and a slight change between the bottom and upper parts of the studied sections are indicated by these profiles.

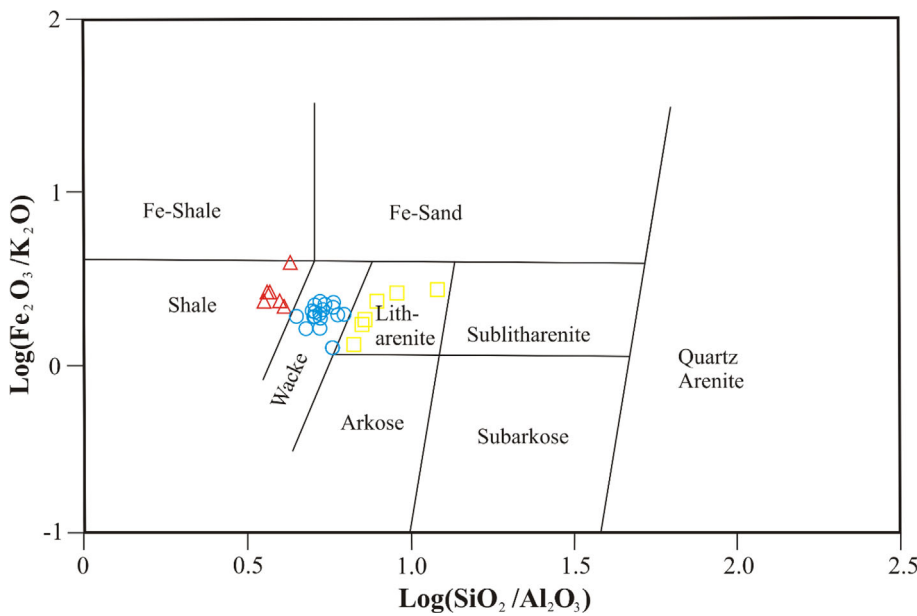


FIGURE 8 Discrimination of lithotypes using $\text{Log}(\text{SiO}_2/\text{Al}_2\text{O}_3)$ vs. $\text{Log}(\text{Fe}_2\text{O}_3/\text{K}_2\text{O})$ Herron (1988) proposed the classification of lithotypes of the studied sediment samples.

7.4 ppm, respectively). Y and Nb were enriched in shale compared with wacke and litharenite.

5 | DISCUSSION

5.1 | Landscape evolution and habitation sites

Facies characteristics (Figure 2a,b) and the textural information (Figure 4) suggested calcrete as the initial landscape/soil surface, over which the river channel sand deposits were superimposed. They were followed towards the top by overbank deposit (flooding and/or channel avulsion), floodplain (seasonal overflow), natural levee (building of banks by overbank flow and stabilization of the banks), flood deposit (bank breach and overland flow above the natural levee surface, which means, perhaps a catastrophic flood) and flood plain (stabilization of the channel flow and seasonal overflow). Both the lithologies and textural properties provided evidence of these depositional-erosional-avulsion events. Together, their stratigraphic variations suggested that the major shifts of the trunk channel of the Vaigai River with flood events perhaps marooned/buried/destroyed the ancient habitation sites that forced the inhabitants to abandon old sites and led to the reestablishment of newer ones.

Despite all the sediment samples falling in the riverine fields (Figure 5a,b) without exception, their depositional environments (Figure 5d) varied braided bars and point bars. Their poor-moderate sorting character, together with other observations and characteristics, suggested episodic excessive sediment supply within a short distance and short duration that could have been a response to high-intensity, short-duration rainfall in the catchments. The energy conditions were also variable, not typical of a normal fluvial environment, as indicated by the plot of all the samples in the region next to the river process, but away from quite-water and wave process fields (Figure 5c), suggestive of high-energy, unidirectional flow (Ramkumar, 2007; Ramkumar et al., 2000, 2015). The scattered nature of the sample fields might suggest highly variable depositional energy. Except few near the C-S line, the samples generally fall within the field of 'rolling and suspension' (Figure 5e). It suggested most of the samples representing periodic floods, during which sediments were brought under turbulent flow and deposited when peak flows dwindle/recede (Ramkumar, 2009; Ramkumar et al., 2015; Sridhar, 2007). Samples near the C-S line represented the fluidized alluvial fill capping with immature sediments, cemented with calcareous material. This bimodality was also reflected in the sediment size distribution. The sediment granulometry and sediment size parameter-based discrimination diagrams broadly followed the depositional conditions inferred from lithofacies and sedimentary structure characteristics. Together they indicated climatic extremes forced the abandonment of ancient habitation sites and their subsequent shift to other regions near the channel course unaffected by the flooding/marooning.

This information points to the fact that there existed an inevitable dependence of the ancient societies from South India on the river banks and the flood plains for settlements and livelihood. However,

the lack of knowledge about extreme climatic events possibly caused the decimation. The studies on the causal link between extreme climatic events and impacts on the habitation sites of ancient societies are at a nascent stage and only a broader perspective, however speculative, may be made with the available data and reports elsewhere. Even at recent history/contemporary society, Soubry et al. (2020) documented that farmers are at the forefront of mitigating climate change effects on agriculture, albeit most of the scientific literature does not contemplate their role. In this context, the present study attempts to document the prevalence of extreme event and, with the available chronological, facies, geochemical and climatic proxies, makes an effort to link with shifting of habitation site on a spatial-temporal scale. Nevertheless, more evidence and data also from other known civilizational sites and river basins are awaited in order to verify and reinforce this perspective. Natural climate change as well as extreme weather events such as floods and droughts exert control over erosion-transportation-deposition processes and impact the landscape development (Bookhagen et al., 2005). Human responses to these climatic fluctuations varied considerably from region to region. In a study involving the faunal analyses and isotopic data in tooth enamel from Gujarat (India), the lack of any significant change in pastoral land-use practices during the drought intervals indicated considerable resilience on the part of local pastoral producers (Chase et al., 2020).

5.2 | Tectonic setting and dynamics

The spatial, temporal and relative contributions of stratigraphic variations in facies and textural characteristics are not explicit. In this context, the examination of the tectonic and climatic events was carried out by plotting the geochemical data in the discriminant diagram of Roser and Korsch (1988), Figure 9a). All the samples in the active continental margin and oceanic island-arc margin fields affirmed tectonic dynamics in the study area as enumerated in the regional setting section. However, the samples plotted in multidimensional diagrams of Verma and Armstrong-Altrin (2016) that use the isometric log-ratio transformation of both major and trace elements showed most of the samples in passive margin and few (3 samples of litharenite and 2 samples of wacke) in the active margin (Figure 9b). The trace elements-based discriminant diagram (Figure 9c) also showed the samples in the active margin (8 samples of wacke and litharenite) and passive margin (remaining wacke and shale). The La-Sc-Zr/10 ternary plot (Figure 9d) also indicated continental island-arc and passive continental margin, and the plot of La-Th-Sc (Figure 9e) showed active and passive margins as possible tectonic settings. Collectively, all these discriminant diagrams suggested active continental margin and passive margin as the dominant tectonic settings. Also, the index of compositional variability (ICV) values is mostly >1 (1.17 to 14.24 in the calcrete sample) in the studied sediments indicating the non-mature nature and referring to tectonically active setting (Cox et al., 1995). This interpretation is in conformity with the landscape evolution model of Ramkumar et al. (2019) that envisaged tectonically active and quiescent episodes

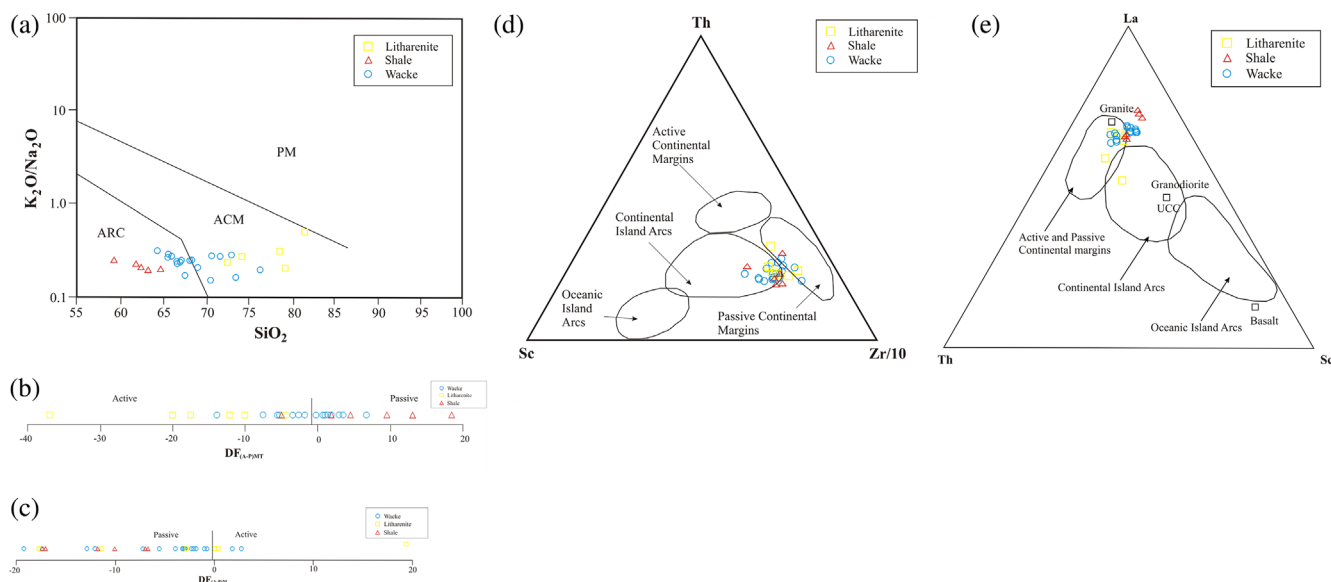


FIGURE 9 Discrimination of tectonic setting based on geochemical data. (a) K_2O/Na_2O versus SiO_2 diagram (after Roser & Korsch, 1988). Plot of sediments in two fields, namely, island arc and active continental margin are observable. (b) Major elements-based multidimensional discriminant function diagram (after Verma & Armstrong-Altrin, 2016) showing the plot of the samples in active and passive continental margin fields. (c) Major and trace elements-based multidimensional discriminant function diagram (after Verma & Armstrong-Altrin, 2016). (d) Th–Sc–Zr/10 ternary plot (after Bhatia & Crook, 1986). (e) La–Th–Sc ternary plot (after Bhatia & Crook, 1986). Together, these diagrams show the episodic prevalence of tectonic activism amidst tectonic quiescence. It can be implicated together with the interpretations based on granulometry and facies as subdued nature of tectonic influence and dominant control of climatic cycles and extreme climatic events over the location, establishment, survival and abandonment of habitation sites.

and evolution of the river basins of southern India, including the Vagai River Basin in five stages of tectono-morphological and climatological dominance.

5.3 | Palaeo-weathering and source rocks

Within tectonic settings varying from stable to active and later quiescent, the regional climatological signals were examined through the changes in weathering regimes of the source and depositional sites (e.g. Menier et al., 2017). Weathering is measured from the rate of alteration of primary minerals (crystalline rock) to secondary oxides (clays) (Nesbitt et al., 1997; Nesbitt & Young, 1984). It mobilizes elements of alkali and alkaline earth metals such as Na, K, Ca and Mg (Gu, 1994; Nesbitt & Young, 1982) and enrich immobile elements such as Al, Ti, Sc, Zr, Hf, Th, Y and REEs. In this regard, the comparable ranges of CIA (53–61 for wacke; 52–69 for litharenite; and 59–63 for shale) suggested low to moderate chemical weathering. Prevalences of initial short-term changes followed by near-steady state weathering were also indicated by stratigraphic changes in CIA (Figure 7). PIA estimated the abundances of secondary aluminous clay compared with the primary plagioclase (Nagarajan et al., 2015; Nesbitt & Young, 1982) and suggested prevalence of moderate weathering in the source region (66–77 in wacke; 65–86 in litharenite; 74–78 in shale) and comparable with CIA.

In order to ascertain the contributions of compositional variations of source rocks, the ternary plots of A–CN–K ($A = Al_2O_3$, $CN = CaO^*$

+ Na_2O , $K = K_2O$) and A–CNK–FM ($A = Al_2O_3$, $CNK = CaO^* + Na_2O + K_2O$, $FM = Fe_2O_3 + MgO$) were employed (Nesbitt & Young, 1984, 1989; Nesbitt and Wilson (1992). The samples along a linear trend parallel to the A–CN line in the A–CN–K plot suggested a possible provenance with the ratio of plagioclase and K-feldspar similar to the granodiorite–granite (Figure 10a). It also revealed the absence of K-metasomatism. A–CNK–FM plot also supported the interpretation of low to moderate weathering nature (Figure 10b).

The single-element mobility during incongruent weathering was estimated by comparing it with non-mobile elements (in this case Al, Gaillardet et al., 1999; Garzanti et al., 2013) and the results show the following order:

$$\alpha^{Al}Cs > \alpha^{Al}Na > \alpha^{Al}Rb > \alpha^{Al}Mg > \alpha^{Al}Ca > \alpha^{Al}K > \alpha^{Al}Sr > \alpha^{Al}Fe > \alpha^{Al}Ba.$$

Higher mobilities were recorded for Cs and Na. According to Nesbitt et al. (1980), Rb and Cs have large ionic radii, and they are retained in weathered products during chemical weathering. Ca and Na also behave similarly during chemical weathering. In addition, other divalent cations, i.e., Mg, Ba and Sr become mobile during chemical weathering (Middelburg et al., 1988; Nesbitt et al., 1980; Zhao et al., 2015). In the present study, the mobility of Cs and Na remained lower in specific depths (Cs at K24, K26–K27 and K1; River channel and modern floodplain environment). Caesium is strongly adsorbed onto clay particles and clay-containing soils (Jolin & Kaminski, 2016) and its depletion may indicate either a low concentration recorded or caesium might be leached during weathering and other events.

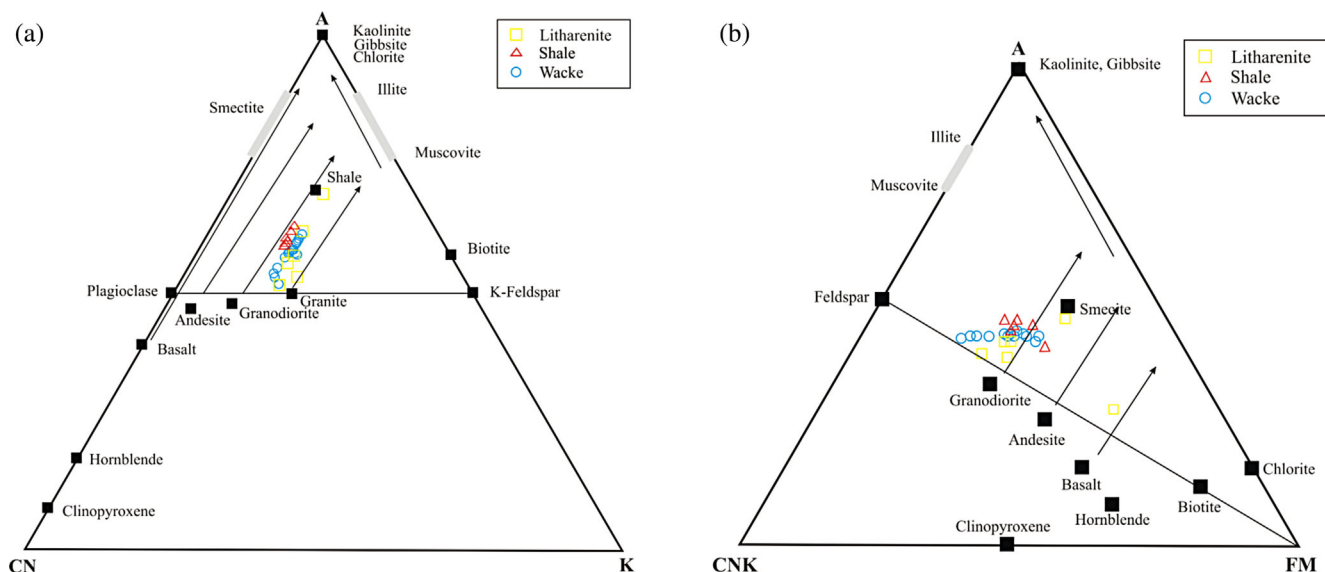


FIGURE 10 Weathering trends. (a) The A-CN-K ternary diagram (after Nesbitt & Young, 1982, 1984) is suggestive of low to moderate weathering and granodiorite source rock for the sediment samples studied. (b) The A-CN-K-FM ternary diagram (after Nesbitt & Wilson, 1992) affirms the previous interpretation of weathering trend and source rock.

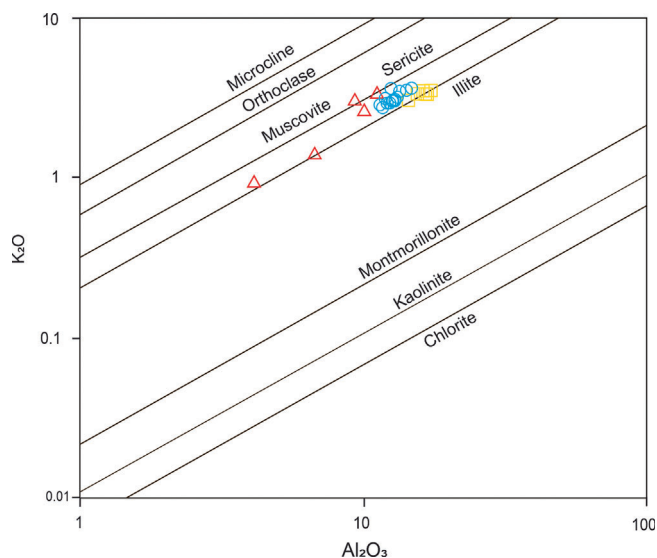


FIGURE 11 Plot of Al_2O_3 vs K_2O . Note that the sediments mainly fall nearer to sericite and illite rather than other clay minerals.

Amongst the alkaline elements, Cs shows high mobility, which may be controlled by clay minerals such as illite, smectite and vermiculite since they exhibit high selectivity for Cs (Latrille & Bildstein, 2022; Smith & Comans, 1996). However, in illite frayed edge sites Cs can be sorped. $\alpha^{137}\text{Cs}$ does not show any correlation with other elements used for calculating mobility factor except a slight positive correlation with $\alpha^{244}\text{Mg}$. Thus, Cs may be controlled by illite/muscovite type of clay minerals and other secondary minerals, in addition to other rock-forming minerals (i.e. beryl and K-feldspar). According to the Al_2O_3 vs K_2O plot, the sediments mainly fall nearer to sericite and illite rather than other clay minerals (Figure 11). Cs is also controlled by Cs- and

Sc-bearing arsenates, which were recorded in five samples. Thus, the high Cs mobility is due to their association of illite with frayed edge sites in selected samples and arsenates while less content of Cs in other samples is related to the rock-forming minerals (i.e. beryl and feldspars). This is supported by the XRD results for the Keezhadi pit samples (Table S1). Furthermore, the high Zr, Hf and Th in specific depths (K24-K26, K19-K21 and K1-K3) indicated enrichments of heavy minerals, possibly by the peak discharge (flood event) and sorting effect in the river (McLennan & Taylor, 1991; Overarea et al., 2021). In addition, the enrichment of Ca can be post-depositional. Both Ca and Na showed inverse trends at the bottom of the section, which may indicate mass conservation during the chemical weathering at the source region, as the enrichment of immobile elements may be balanced by the depletion of mobile elements (Zhao et al., 2015).

5.4 | Climate

Ga/Rb vs Sr/Cu plot has been proposed to constrain paleoclimate regime based on the fact that Ga is associated with fine aluminosilicate fraction (i.e. kaolinite) and Rb is associated with illite (Roy & Roser, 2013; Xie et al., 2018). So, high values of Ga/Rb ratios represent a humid climate while lower values mirror the cold and dry climate conditions (Roy & Roser, 2013). Most samples in cool/arid category, except for one sample (K29), indicate predominantly arid conditions in the river basin (Figure 12a, Xie et al., 2018). The plot of $\text{Al}_2\text{O}_3 + \text{Na}_2\text{O} + \text{K}_2\text{O}$ against SiO_2 (Figure 12b, Suttner and Dutta, 1986) also suggested arid conditions. Samples K30 and K29 at the bottom of the profile are palaeosols (calcrete), representing humid conditions, while the rest of the samples represent arid climate. This

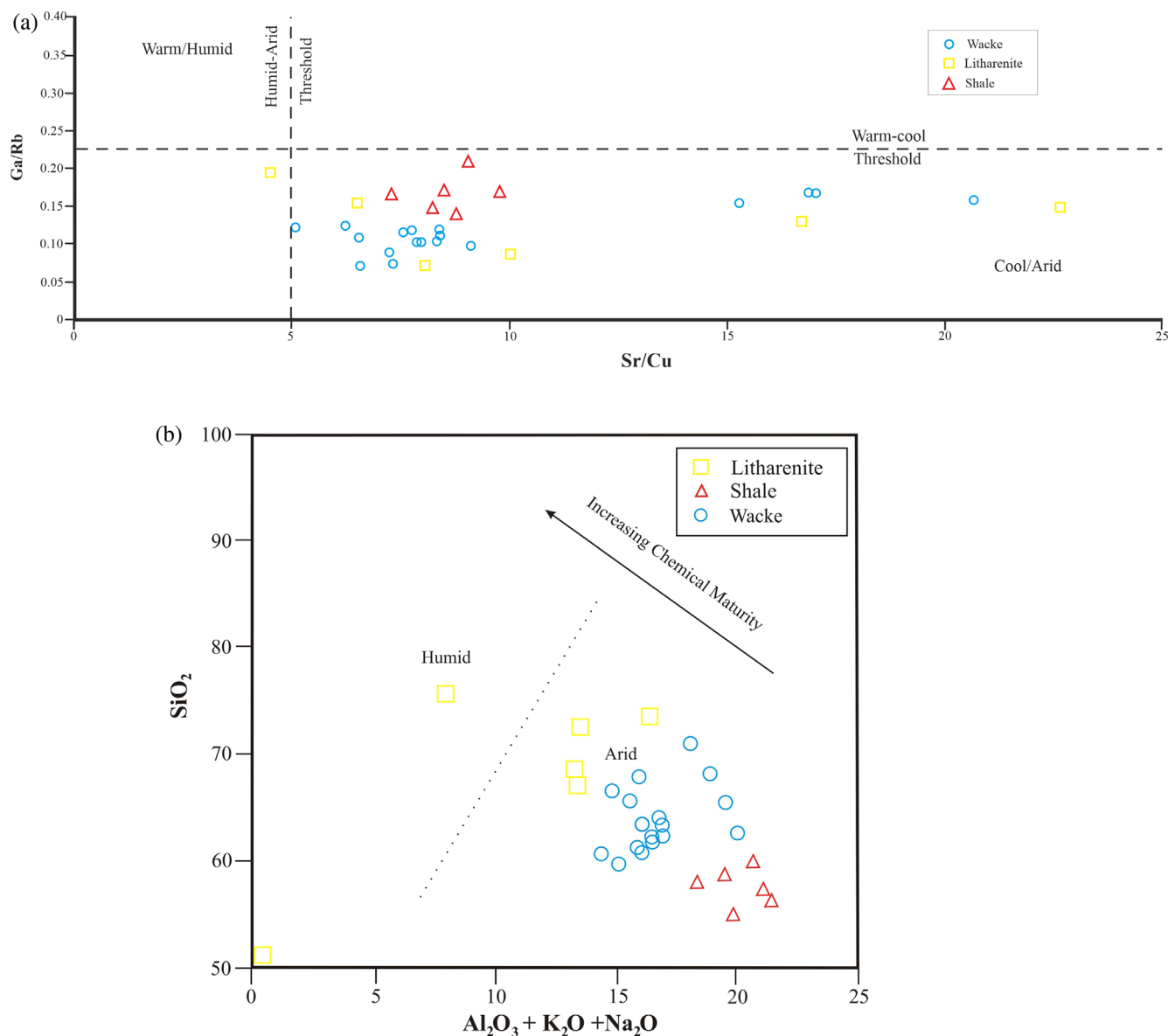


FIGURE 12 Interpretation of palaeoclimate based on elemental ratios. (a) Plot of Sr/Cu against Ga/Rb plot (after Xie et al., 2018) shows all the samples falling in the arid climatic conditions except one. (b) Plot of Al₂O₃ + Na₂O + K₂O vs. SiO₂ plot (after Suttner & Dutta, 1986) showing all the samples in the arid climatic conditions except two. Together, the regional prevalence of arid climate, seasonal normal flows and occurrences of perturbations in the flow conditions as a result of extreme climatic conditions and associated channel avulsion, marooning and or burial under flood deposits could be interpreted along with the facies and granulometric characteristics of the studied samples.

suggests a shift from a humid to an arid climate and followed by channel shift and deposition of river sands over calcrete, with no major basin-scale climate changes afterward. The studies of alluvial and flood deposits over three dozen sites in the Indian Peninsula indicate that the variations in the monsoon strengthen the fluvial activity during the Holocene (Kale, 2022). The flooding and channel avulsion events recorded might be of high-intensity, short-term events, which are typical of the east-flowing Peninsular rivers of southern India (Ramkumar et al., 2016; Ramkumar et al., 2019, 2021). These observations and inferences are also in conformity with the nature of the polynomial curve of the textural parameter of Agaram pit (Figure 4).

The clay minerals are products of erosion and weathering of fresh rocks and serve as indicators of palaeoclimatic evaluation (Chaudhri & Singh, 2012). Playter et al. (2018) used a set of element ratios to differentiate the clay mineral changes in a stratigraphic profile. The ratio of Na/Al and Ga/Rb represent smectite and kaolinite contents, whereas the K/Rb, Zn/Sc, K/Al and Rb/Al ratios indicate illite content. The bulk mineralogy of Keezhadi samples shows illite/muscovites than other types of clay minerals. Accordingly, the intense and copious rainfall during the deposition of bottom sediments and relatively meager rainfall thenceforth were indicated by these ratios. In addition, higher Na/Al suggestive of the presence of smectite in the sediments of the upper part of the profile indicated a dry period with intense

evaporation (Garzanti et al., 2013; Velde, 1995); however, clay mineralogy is required to confirm this. The rest of the samples in the cool and dry climatic conditions were represented by the low K/Rb, high Zn/Sc and Rb/Al from natural levee to sandy loam floodplain.

6 | IMPLICATION OF CLIMATE ON SHIFTING OF HABITATION

The kankar (calcrete) surfaces have been used as habitation sites since the early Holocene or Microlithic times (Arjun, 2022; Field et al., 2007; Ramkumar et al., 2021). These sites supported human activities and seldom wreaked havoc and forced the habitat to shift or marooned the settlements (Patterson et al., 2010; Ramkumar, Balasubramani, et al., 2022). In a comprehensive review of the archaeological and climatological research, Laskar and Bohra (2021) related the variability of the Indian summer monsoon (ISM) on the rise with the fall of ancient Indian civilizations for the most part of the ongoing interglacial period, i.e. the Holocene. The majority of the paleoclimate reconstruction studies identified ISM intensification between 9 and 5 ka and inferred a general aridity trend after 4 ka (Banerji et al., 2021; Misra et al., 2019). Evidence across the world has also shown that catastrophic flood events have buried ancient habitats in floodplains (Gao et al., 2023; Sridhar, 2007; Wang et al., 2016). These studies demonstrate that global climatic epochs have varying impacts on monsoonal activity across different regions in India. Nevertheless, assessing their influence on human settlement and dispersion necessitates high-resolution archaeological and climate change data (Laskar & Bohra, 2021). Flooding is a common phenomenon in all the Indian rivers during the peak of monsoon and the climatic variability at the global/regional scale might have played a major role in the catastrophic flood events over the Holocene (Kale et al., 2010). Extreme floods in river systems alter the channel hydraulics and impact short- and long-term erosion/deposition patterns in the fluvial systems (Heritage et al., 2004; Ramkumar et al., 2015). Changes in rainfall patterns in catchments are potentially linked with topographic evolution within the channel and attendant marooning and burial of ancient habitats in the floodplains (Ramkumar, Balasubramani, et al., 2022; Wulf et al., 2010). The avulsion of a river to a new course is influenced by several factors including increasing sinuosity, sea level change, neotectonism, vegetation and hydrodynamic conditions (Jones & Schumm, 1999). Given cognizance of these, it is perceivable that the burial of habitations in the basin might have been related to extreme floods induced by the changes in the climatic system. Compilation of present observations and the data from Ramkumar et al. (2021); Ramkumar, Balasubramani, et al. (2022) allowed recognition of six habitation sites/surfaces of urbanism, religio-cultural, industrial, leisure activities and cohabitation of multiple societal groups in the Vaigai River Basin. Accordingly, this basin has been inhabited by humans at least since the early to mid-Holocene, as shown by the presence of modern habitations, buried habitation phases, and microlithic tools. After the nomadic microlithic period, the first habitation surface in the kankar

(known as habitation surface 1 or HS-1) was constrained between 5627 and 5370 BCE. It was followed by the second habitation surface (HS-2), both in the Keezhadi pit (3346–2589 BCE) as well in the Agaram pit (3307–2878 BCE). The radiocarbon dates for 23 principal sites have also shown the emergence of Neolithic villages in various geographical pockets of South India during this period (Arjun, 2022). The third dwelling surface (HS-3) was dated to 1613–1414 BCE, and the fourth habitation surface (HS-4) was demarked in the sediments deposited between 752 and 406 BCE. This habitation surface is aligned with the Iron Age (1200–300 BCE) of South India and is known for its burial tradition (Moorti, 1994). The fifth habitation-colonization (HS-5) was constrained to 555–644 CE, while the sixth habitation (HS-6) was buried in sediments deposited between 1167 and 1269 CE. All of these have been summarized and presented in Figure 3.

These perceived and inferred habitation-flourishing-marooning-demise-reestablishment events are interpreted to have been under the controls of regional climatological dynamics and attendant geomorphological evolution, based on the facies, granulometric and geochemical proxies and these inferences are examined in the light of available, documented speleothem records of the Indian subcontinent. Links between the climatic changes and expansion of agriculture in the Indus Basin during 10,000 and 7000 cal. years BP were reported by Gupta (2004). Speleothem proxy records from Mawmluh Cave, northeastern (NE) India, suggested warm intervals suggesting increased ISM strength during the early Holocene (~10,000 to 6500 years BP) that in turn show, correspond to increased river discharge to the Bay of Bengal (BoB) (Dutt et al., 2015; Govil & Naidu, 2011). In the BoB, the moisture source for the ISM, an ~3.2–3.5°C increase in sea surface temperature (SST) between the last glacial maximum and the Holocene and a +1.4°C SST shift between the Younger Dryas and the Holocene have been documented (Govil & Naidu, 2011; Lechleitner et al., 2017; Rashid et al., 2007; Rashid et al., 2011). The documented first habitation in the Vaigai Civilization occurred during this period. The strengthened Holocene ISM (10,000–7000 years BP.) is followed by a sudden decrease at 6500 years BP, indicating a weak phase of ISM (Dutt et al., 2015; Gupta et al., 2003). A recent study of the lake sediments by Rawat et al. (2021) found that there is a cyclic strengthening of precipitation that were recorded from ~5930 to 3950, ~3380–2830, ~2610–1860, ~1050–760 and ~320 cal year BP to present. The HS-1, HS-2 and HS-5 of this study area are falling well in these high precipitation intervals. The increased river discharge, as revealed by the speleothem records, may be linked with the demolition/destruction of the first habitation site by flooding and channel avulsion (Ramkumar, Balasubramani, et al., 2022). The fining upward (from coarse sand to fine sand) sequence of river channel sediments at Agaram suggested an avulsion threshold. The coral colony at ca. 7.3 ka at Rameshwaram suggested an eustatic change of up to 3 m on the southeast coast of India (Banerjee, 2000). Banerji et al. (2021) observed the high sea stands between 6430 and 4390 BP through a dating of core samples obtained from a lake in South India. This interval of sea level highstand might have caused a reduction in the slope of the Vaigai River, thus helping in the stream avulsion. The

proxy records from the Indian subcontinent indicate that the ISM weakened significantly (Berkelhammer et al., 2012; Dixit, Hodell, & Petrie, 2014; Kathayat et al., 2017; Laskar & Bohra, 2021; Laskar, Yadava, Ramesh, et al., 2013; Nakamura et al., 2016; Staubwasser et al., 2003) after the demobilization of first habitation and was characterized by drought for two to three centuries (e.g., Berkelhammer et al., 2012; Dixit, Hodell, Sinha, & Petrie, 2014; Nakamura et al., 2016). Other smaller magnitude climate events also impacted the ISM during the late Holocene (Laskar et al., 2010; Laskar & Bohra, 2021; Laskar, Yadava, Ramesh, et al., 2013; Laskar, Yadava, Sharma, & Ramesh, 2013) could possibly be linked to the short duration, high-intensity flooding and channel avulsion events interpreted by our study. However, very-high-resolution chronological control and climatic proxies are necessary in order to make this inference affirmatively. In the nearby Cauvery River, Ramkumar et al. (2018) reported that the tectonic line provided continuous accommodation space to flood deposits for new channel courses and flow regimes. High values of Al and Fe (K 24–26) (Figure 7) at Keezhadi pit-2 indicate more runoff (flood) in the channel. Similarly, the Keezhadi pit-1 (KLMB 5) showed two peaks in the frequency curve, which indicated the transport of sedimentary material from different sources or possibly different exhumation surfaces (Ramkumar & Berner, 2015) during times of intense erosion–deposition that normally occurs during extreme climatic events (Ramkumar, 2015) and/or as a result of variations in flow/sediment dynamics (Sun et al., 2003). Ramkumar et al. (2021) also documented higher mobility of mobile (Na) and non-mobile elements (Cs) in certain depths (K24, 26–27) due to flash floods. An increment of Al, Fe, CIA and Rb/Sr in sample K19 indicated high hydrodynamic conditions during the second habitation. The third habitation was after the flooding and abandoning during the second habitation, which may be resettlement after normalcy returned. Banerji et al. (2021) witnessed poor hydroclimatic conditions caused by weak monsoon during 2500–1000 BP from the geochemical proxies while conspicuous increase in the monsoon after 1000 BP which possibly led to a warm and wet climate after 1000 cal yr BP. Therefore, the fourth habitation was also perished by the flood (Ramkumar, Balasubramani, et al., 2022). Very fine and very coarse-skewed sediments at depths of K12–K8 indicated high-energy conditions similar to a flood event. Thus, the perceived low-intensity climatic events as recorded in the speleothem data may be related to these floods of second, third and fourth flooding–marooning surfaces. The fifth habitation site was abandoned by vegetation growth, avulsion channel again due to the reduction of precipitation, indicated by low Al, and Fe, and CIA values and high Ca/Mg ratio (Figure 7). Reduction of depositional energy conditions and development of mudflat–pointbar–marsh/vegetation led to the deposition of organic carbon-rich layer that provided an age of 689 ± 24 BP. Further shifting of the channel from Agaram towards the present-day course might have occurred thenceforth. These could be corroborated with the speleothem ^{18}O records from the Bay of Bengal region suggesting ISM enhancement during 2.1–0.8 kyr BP, and during the transition from the Medieval Climate Anomaly to the Little Ice Age (0.8–0.4 kyr BP) (Laskar & Bohra, 2021; Laskar,

Yadava, Ramesh, et al., 2013). It is also pertinent to note here the study of Chauhan et al. (2010) who inferred high contribution of chlorite and kaolinite into the Bay of Bengal during 2.2–1.8 ka and the reduced K/C ratio was a reflection of high monsoon precipitation. Similar to our findings, Mohapatra et al. (2019) observed anthropogenic activities in the adjacent Cauvery delta plains during the mid-Holocene (7000–5000 BP) through the pollen records. They have linked pollen records with agriculture and inferred that the riverine environment becoming more suitable for human settlement in the mid-Holocene. Together, although not exactly correlatable, the periods of significant climatic shifts, intense and weakening of monsoon and flood discharge events as documented by published proxy records of the continental as well marine regions. It is reiterated that while a general corroboration could be established with the available data and very-high resolution chronological and climate proxy records of the habitation sites need to be documented for precise correlation.

7 | CONCLUSIONS

Sedimentary strata of the Vaigai River Basin in South India preserve evidence of habitational sites from the microlithic era until the historic past. Spatial and chronological constraining of these civilizational sites/habitation surfaces also evidence their episodic marooning/shifting characteristics, albeit on a transitional-sudden catastrophic scale. Integrated analyses of facies, texture, mineralogy, geochemistry and constraining with chronological data have revealed the prevalent episodic/multiple events of sudden and gradual shifts in the channel courses that enforced concomitant abandonment and establishment(s) of newer habitation sites. While few of the events were cyclic, others were found to be sudden and catastrophic. The influence of the 4.2-ka-like event was indirectly recognized, and it requires more details and reaffirmation. However, the present study documented the evidence of global climatic events as well as regional and local-scale geological, tectonic and climatic events and on the evolution of the Vaigai civilization in South India.

AUTHOR CONTRIBUTIONS

Mu. Ramkumar: Supervision, conceptualization, data curation, investigation, interpretation, writing original draft, editing. **R. Nagarajan:** Geochemical analysis, interpretation, data curation, editing and review. **K. J. Juni:** Sample analysis, data analysis, interpretation, graphic preparation. **A. Manobalaji:** Sample collection, processing of samples and calculation, interpretation. **K. Balasubramani:** Modified, edited & drafting text. **Priyadarsi D. Roy:** Review & editing. **K. Kumaraswamy:** Investigation & data analyses. **A. L. Fathima:** Data analysis, interpretation. **Athira Pramod:** Graphic preparation, data analysis. **R. Sharveen:** XRD analysis and interpretation. **S. Abdul Rahman:** GIS analyses & interpretation. **N. A. Siddiqui:** Review & editing. **D. Menier:** Review and Editing. **Rajveer Sharma:** Carbon dating and interpretation.

ACKNOWLEDGEMENTS

The authorities of Periyar University and the Department of Archaeology, State Government of Tamil Nadu, are thanked for granting the necessary administrative permission to conduct field investigations and sampling campaigns. The MoU's signed between the Periyar University and the University of South Brittany, France, Curtin University Malaysia, and Universiti Teknologi Petronas facilitated collaborative work, and the authors are thankful for the same. The authors are thankful to IUAC for extending AMS facility for ^{14}C funded by the Ministry of Earth Science (MoES), Government of India (reference numbers MoES/16/07/11(i)-RDEAS and MoES/P.O. (Seismic)8(09) – Geochron/2012). The authors are thankful to Malvern Panalytical for providing two High-Score software licenses for a year.

PEER REVIEW

The peer review history for this article is available at <https://www.webofscience.com/api/gateway/wos/peer-review/10.1002/gj.4919>.

DATA AVAILABILITY STATEMENT

The data that support the findings of this study are available on request from the corresponding author. The data are not publicly available due to privacy or ethical restrictions.

ORCID

Mu. Ramkumar  <https://orcid.org/0000-0002-4038-6978>

R. Nagarajan  <https://orcid.org/0000-0003-3495-899X>

K. J. Juni  <https://orcid.org/0000-0003-2288-1016>

K. Balasubramani  <https://orcid.org/0000-0003-0671-1033>

Priyadarsi D. Roy  <https://orcid.org/0000-0003-3284-8762>

S. Abdul Rahman  <https://orcid.org/0000-0002-9283-471X>

N. A. Siddiqui  <https://orcid.org/0000-0002-6703-0699>

REFERENCES

- Arjun, R. (2022). Prehistoric settlement developments in the multi-period sites of South India. *Brahmagiri Hill L'Anthropologie*, 126(5), 103026.
- Banerjee, P. K. (2000). Holocene and late Pleistocene Relative Sea level fluctuations along the East Coast of India. *Marine Geology*, 167, 243–260.
- Banerji, U. S., Shaji, J., Arulbalaji, P., Maya, K., Vishnu Mohan, S., Dabhi, A. J., Shivam, A., Bhushan, R., & Padmalal, D. (2021). Mid-late Holocene evolutionary history and climate reconstruction of Vellayani lake, South India. *Quaternary International*, 599–600, 72–94.
- Bar-Matthews, M., & Ayalon, A. (2011). Mid-Holocene climate variations revealed by high-resolution speleothem records from Soreq cave, Israel and their correlation with cultural changes. *The Holocene*, 21, 163–171.
- Berkelhammer, M., Sinha, A., Stott, L., Cheng, H., Pausata, F. S., & Yoshimura, K. (2012). An abrupt shift in the Indian monsoon 4000 years ago. *Climates, Landscapes, and Civilizations*, 198, 75–88.
- Bhatia, M. R., & Crook, K. A. W. (1986). Trace element characteristics of graywackes and tectonic discrimination of sedimentary basins. *Contributions to Mineralogy and Petrology*, 92, 181–193.
- Bock, B., McLennan, S. M., & Hanson, G. N. (1998). Geochemistry and provenance of the middle Ordovician Austin Glen member (Normanskill formation) and the Taconian orogeny in New England. *Sedimentology*, 45, 635–655.
- Bookhagen, B., Thiede, R. C., & Strecker, M. R. (2005). Abnormal monsoon years and their control on erosion and sediment flux in the high, arid northwest Himalaya. *Earth and Planetary Science Letters*, 231, 131–146.
- Bronk Ramsey, C. (2009). Bayesian analysis of radiocarbon dates. *Radiocarbon*, 51, 337–360.
- Chase, B., Meiggs, D., & Ajithprasad, P. (2020). Pastoralism, climate change, and the transformation of the Indus civilization in Gujarat: Faunal analyses and biogenic isotopes. *Journal of Anthropological Archaeology*, 59, 101173. <https://doi.org/10.1016/j.jaa.2020.101173>
- Chaudhri, A. R., & Singh, M. (2012). Clay minerals as climate change indicators – A case study. *American Journal of Climate Change*, 1, 231–239.
- Chauhan, O. S., Dayal, A. M., Basavaiah, N., & Kader, U. S. A. (2010). Indian summer monsoon and winter hydrographic variation over past millennia resolved by clay sedimentation. *Geochemistry, Geophysics, Geosystems*, 11(9), Q09009. <https://doi.org/10.1029/2010GC003067>
- Chetty, T. R. K. (2021). Multiple thrust systems from the southern granulite terrane, India: Insights on Precambrian convergent margin tectonics. *Journal of Asian Earth Sciences*, 208, 104674.
- Cox, R., Lowe, D. R., & Cullers, R. (1995). The influence of sediment recycling and basement composition on evolution of mudrock chemistry in the southwestern United States. *Geochimica et Cosmochimica Acta*, 59, 2919–2940. [https://doi.org/10.1016/0016-7037\(95\)00185-9](https://doi.org/10.1016/0016-7037(95)00185-9)
- de Menocal, P. (2001). Cultural responses to climate change during the late Holocene. *Science*, 292, 667–673.
- Dixit, Y., Hodell, D. A., & Petrie, C. A. (2014). Abrupt weakening of the summer monsoon in Northwest India 4100 Yr ago. *Geology*, 42(4), 339–342.
- Dixit, Y., Hodell, D. A., Sinha, R. C. A., & Petrie, C. A. (2014). Abrupt weakening of the Indian summer monsoon at 8.2 Kyr B.P. *Earth and Planetary Science Letters*, 391, 16–23. <https://doi.org/10.1016/j.epsl.2014.01.026>
- Drury, S. A., Harris, N. B. W., Holt, R. W., Reeves-Smith, G. J., & Wightman, R. T. (1984). Precambrian tectonics and crustal evolution in South India. *The Journal of Geology*, 92, 3–20.
- Dutt, S., Gupta, A. K., Clemens, S. C., Cheng, H., Singh, R. K., Kathayat, G., & Edwards, R. L. (2015). Abrupt changes in Indian summer monsoon strength during 33,800 to 5500 years B.P. *Geophysical Research Letters*, 42(13), 5526–5532.
- Fedo, C. M., Nesbitt, H. W., & Young, G. M. (1995). Unraveling the effects of potassium metasomatism in sedimentary rocks and paleosols, with implications for paleoweathering conditions and provenance. *Geology*, 23, 921–924.
- Field, J. S., Petraglia, M. D., & Lahr, M. M. (2007). The southern dispersal hypothesis and the south Asian archaeological record: Examination of dispersal routes through GIS analysis. *Journal of Anthropological Archaeology*, 26(1), 88–108.
- Folk, R. L., & Ward, W. C. (1957). Brazos River bar: A study in the significance of grain size parameters. *Journal of Sedimentary Research*, 27, 3–26.
- Friedman, G. M. (1967). Dynamic processes and statistical parameters compared for size frequency distribution of beach and river sands. *Journal of Sedimentary Research*, 37, 327–354.
- Gaillardet, J., Dupre, B., & Allegre, C. J. (1999). Geochemistry of large river suspended sediments: Silicate weathering or recycling tracer? *Geochimica et Cosmochimica Acta*, 63, 4037–4051.
- Gao, P., Santosh, M., Yang, C.-X., Kwon, S., & Ramkumar, M. (2021). High Ba–Sr adakitic charnockite suite from the Nagercoil block, southern India: Vestiges of Paleoproterozoic arc and implications for Columbia to Gondwana. *Geoscience Frontiers*, 12, 101126.
- Gao, W., Yuan, H., Pan, Y., Jia, W., Liu, X., & Li, K. (2023). Spatiotemporal variation of human settlement distribution between the Shang and Western Zhou dynasties in relation to flooding in the lower Yellow

- River floodplain, East China. *Journal of Archaeological Science: Reports*, 52, 104260.
- Garzanti, E., Padoan, M., Peruta, L., Setti, M., Najman, Y., & Villa, I. M. (2013). Weathering geochemistry and Sr-Nd fingerprints of equatorial upper Nile and Congo muds. *Geochemistry, Geophysics, Geosystems*, 14, 292–316.
- Ghosh, J. G., Wit, M. J. D., & Zartman, R. E. (2004). Age and tectonic evolution of Neoproterozoic ductile shear zones in the southern granulite terrain of India, with implications for Gondwana studies. *Tectonics*, 23, 1–38.
- Giosan, L., Clift, P. D., Macklin, M. G., Fuller, D. Q., Constantinescu, S., Durcan, J. A., & Syvitski, J. P. (2012). Fluvial landscapes of the Harappan civilization. *Proceedings of the National Academy of Sciences*, 109, E1688–E1694.
- Glaister, R. P., & Nelson, H. W. (1974). Grain size distributions, an aid in facies identification. *Bulletin of Canadian Petroleum Geology*, 22, 203–240.
- Govil, P., & Naidu, P. D. (2011). Variations of Indian monsoon precipitation during the last 32 kyr reflected in the surface hydrography of the Western Bay of Bengal. *Quaternary Science Reviews*, 30(27–28), 3871–3879.
- Gu, X. X. (1994). Geochemical characteristics of the Triassic Tethys-turbidites in northwestern Sichuan, China: Implications for provenance and interpretation of the tectonic setting. *Geochimica et Cosmochimica Acta*, 58, 4615–4631.
- Gupta, A. K. (2004). Origin of agriculture and domestication of plants and animals linked to early Holocene climate amelioration. *Current Science*, 87, 54–59.
- Gupta, A. K., Anderson, D. M., & Overpeck, J. T. (2003). Abrupt changes in the Asian southwest monsoon during the Holocene and their links to the North Atlantic Ocean. *Nature*, 421, 354–357.
- Heritage, G. L., Large, A. R. G., Moon, B. P., & Jewitt, G. (2004). Channel hydraulics and geomorphic effects of an extreme flood event on the Sabie River, South Africa. *Catena*, 58, 151–181.
- Herron, M. M. (1988). Geochemical classification of terrigenous sands and shales from core or log data. *Journal of Sedimentary Research*, 58, 820–829.
- Huitema, D., & Meijerink, S. (2017). The politics of river basin organizations: Institutional design choices, coalitions and consequences. *Ecology and Society*, 22, 1–16.
- Ingram, R. L. (1970). *Sieve analysis: Procedures in sedimentary petrology*. Wiley.
- Jolin, W. C., & Kaminski, M. (2016). Sorbent materials for rapid remediation of wash water during radiological event relief. *Chemosphere*, 162, 165–171.
- Jones, L. S., & Schumm, S. A. (1999). Causes of avulsion: An overview. *Fluvial Sedimentology VI*, 28, 169–178.
- Juni, K. J., Ramkumar, M., Venugopal, T., Fathima, A. L., & Pramod, A. (2022). Assessment of landscape evolution and spatio-temporal variations in tectonic pulses in the Vaigai River basin, Southern India. *The Indian Geographical Journal*, 97(1), 60–78.
- Kale, V. S. (2022). Holocene regional-scale behavior of the rivers of Indian Peninsula. In: Navnith Kumaran & Padmalal Damodara (Eds.). *Holocene Climate Change and Environment*. pp. 103–129. Elsevier, Amsterdam, Netherlands. <https://doi.org/10.1016/B978-0-323-90085-0.00017-6>
- Kale, V. S., Achyuthan, H., Jaiswal, M. K., & Sengupta, S. (2010). Palaeoflood records from upper Kaveri River, southern India: Evidence for discrete floods during Holocene. *Geochronometria*, 37, 49–55.
- Kathayat, G., Cheng, H., Sinha, A., Yi, L., Li, X., Zhang, H., Li, H. Y., Neng, Y. F., & Edwards, R. L. (2017). The Indian monsoon variability and civilization changes in the Indian subcontinent. *Science Advances*, 3(12), e1701296.
- Kennett, D. J., & Kennett, J. P. (2007). Influence of Holocene marine transgression and climate change on cultural evolution in southern Mesopotamia. This chapter appeared in somewhat different form in the journal of *Island & Coastal Archaeology* 1:67–99 and is used with permission of the Taylor & Francis Group, LLC. In: Anderson, D. G. Maasch, K.A. Sandweiss, D.H. (Eds.) *Climate change and culture dynamics: A global perspective on mid-Holocene transitions*, Elsevier, San Diego, USA, 229–264. <https://doi.org/10.1016/B978-012088390-5.50012-1>
- Laskar, A., Yadava, M., Sharma, N., & Ramesh, R. (2013). Late-Holocene climate in the lower Narmada valley, Gujarat, Western India, inferred using sedimentary carbon and oxygen isotope ratios. *The Holocene*, 23(8), 1115–1122.
- Laskar, A. H., & Bohra, A. (2021). Impact of Indian summer monsoon change on ancient Indian civilizations during the Holocene. *Frontiers in Earth Science*, 9, 709455.
- Laskar, A. H., Sharma, N., Ramesh, R., Jani, R. A., & Yadava, M. G. (2010). Paleoclimate and paleovegetation of lower Narmada Basin, Gujarat, Western India, inferred from stable carbon and oxygen isotopes. *Quaternary International*, 227(2), 183–189.
- Laskar, A. H., Yadava, M. G., Ramesh, R., Polyak, V. J., & Asmerom, Y. (2013). A 4 kyr stalagmite oxygen isotopic record of the past Indian summer monsoon in the Andaman Islands. *Geochemistry, Geophysics, Geosystems*, 14(9), 3555–3566.
- Latrille, C., & Bildstein, O. (2022). Cs selectivity and adsorption reversibility on Ca-illite and Ca-vermiculite. *Chemosphere*, 288, 132582. <https://doi.org/10.1016/j.chemosphere.2021.132582>
- Lechleitner, F. A., Breitenbach, S. F., Cheng, H., Plessen, B., Rehfeld, K., Goswami, B., Marwan, N., Eroglu, D., Adkins, J., & Haug, G. (2017). Climatic and in-cave influences on $\delta^{18}\text{O}$ and $\delta^{13}\text{C}$ in a stalagmite from northeastern India through the last deglaciation. *Quaternary Research*, 88(3), 458–471.
- Li, F., Wu, L., Zhu, C., Zheng, C., Sun, W., Wang, X., Shao, S., Zhou, Y., He, T., & Li, S. (2013). Spatial-temporal distribution and geographic context of Neolithic cultural sites in the Hanjiang River basin, southern Shaanxi, China. *Journal of Archaeological Science*, 40, 3141–3152.
- Macklin, M. G., Woodward, J. C., Welsby, D. A., Duller, G. A. T., Williams, F. M., & Williams, M. A. J. (2013). Reach-scale river dynamics moderate the impact of rapid Holocene climate change on floodwater farming in the desert Nile. *Geology*, 41, 695–698.
- Madella, M., & Fuller, D. Q. (2006). Palaeoecology and the Harappan civilization of South Asia: A reconsideration. *Quaternary Science Reviews*, 25, 1283–1301.
- McIntosh, J. (2007). *The ancient Indus Valley: New perspectives*. ABC-CLIO.
- McLennan, S. M., Hemming, S., McDaniel, D. K., & Hanson, G. N. (1993). Geochemical approaches to sedimentation, provenance, and tectonics. *Geological Society of America Special Paper*, 284, 21–40.
- McLennan, S. M., & Taylor, S. R. (1991). Sedimentary rocks and crustal evolution: Tectonic setting and secular trends. *The Journal of Geology*, 99, 1–21.
- Mehrotra, N., Shah, S. K., Basavaiah, N., Laskar, A. H., & Yadava, M. G. (2019). Resonance of the ‘4.2ka event’ and terminations of global civilizations during the Holocene, in the paleoclimate records around PT Tso Lake, Eastern Himalaya. *Quaternary International*, 507, 206–216.
- Menier, D., Mathew, M. J., Pubellier, M., Sapin, F., Delcaillau, B., Siddiqui, N., Ramkumar, M., & Santosh, M. (2017). Landscape response to progressive tectonic and climatic forcing in NW Borneo: Implications for geological and geomorphic controls on flood hazard. *Scientific Reports*, 7, 457.
- Middelburg, J. J., Van der Weijden, C. H., & Woittiez, J. R. W. (1988). Chemical processes affecting the mobility of major, minor and trace elements during weathering of granitic rocks. *Chemical Geology*, 68, 253–273.

- Misra, P., Tandon, S. K., & Sinha, R. (2019). Holocene climate records from lake sediments in India: Assessment of coherence across climate zones. *Earth-Science Reviews*, 190, 370–397.
- Mohapatra, P., Stephen, A., Prasad, S., Singh, P., & Anupama, K. (2019). Late Pleistocene and Holocene vegetation changes and anthropogenic impacts in the Cauvery delta plains, southern India. *Quaternary International*, 507, 249–261.
- Moiola, R. J., & Weiser, D. (1968). Textural parameters: An evaluation. *Journal of Sedimentary Research*, 38, 45–53.
- Moorti, U. S. (1994). *Megalithic culture of South India: Socio-economic perspectives*. Ganga Kaveri Publishing House.
- Nagarajan, R., Armstrong-Altrin, J. S., Kessler, F. L., Hidalgo-Moral, E. L., Dodge-Wan, D., & Taib, N. I. (2015). Provenance and tectonic setting of Miocene siliciclastic sediments, Sibuti formation, northwestern Borneo. *Arabian Journal of Geosciences*, 8, 8549–8565.
- Nagarajan, R., Armstrong-Altrin, J. S., Kessler, F. L., & Jong, J. (2017). Petrological and geochemical constraints on provenance, paleo-weathering and tectonic setting of clastic sediments from the Neogene Lambir and Sibuti formations, NW Borneo. In R. Mazumder (Ed.), *Sediment provenance: Influences on compositional change from source to sink* (pp. 123–153). Elsevier.
- Nakamura, A., Yokoyama, Y., Maemoku, H., Yagi, H., Okamura, M., Matsuoka, H., & Matsuzaki, H. (2016). Weak monsoon event at 4.2 ka recorded in sediment from Lake Rara, Himalayas. *Quaternary International*, 397, 349–359.
- Nesbitt, H. W., Fedo, C. M., & Young, G. M. (1997). Quartz and feldspar stability, steady and non steady-state weathering, and petrogenesis of siliciclastic sands and muds. *Journal of Geology*, 105, 173–192.
- Nesbitt, H. W., Markovics, G., & Price, R. C. (1980). Chemical processes affecting alkalis and alkaline earths during continental weathering. *Geochimica et Cosmochimica Acta*, 44, 1659–1666.
- Nesbitt, H. W., & Wilson, R. E. (1992). Recent chemical weathering of basalts. *American Journal of Science*, 292, 740–777.
- Nesbitt, H. W., & Young, G. M. (1982). Early Proterozoic climates and plate motions inferred from major element chemistry of lutites. *Nature*, 299, 715–717.
- Nesbitt, H. W., & Young, G. M. (1984). Prediction of some weathering trends of plutonic and volcanic rocks based on thermodynamic and kinetic considerations. *Geochimica et Cosmochimica Acta*, 48, 1523–1534.
- Nesbitt, H. W., & Young, G. M. (1989). Formation and diagenesis of weathering profiles. *The Journal of Geology*, 97, 129–147.
- Overarea, B., Azmya, B., Azmy, K., Garzantic, E., Osokporb, J., Ogbob, O. B., & Awwenagha, E. O. (2021). Decrypting geochemical signatures in subsurface Niger delta sediments: Implication for provenance, weathering and paleo-environmental conditions. *Marine and Petroleum Geology*, 126, 104879.
- Passega, R. (1957). Texture as characteristic of clastic deposition. *American Association of Petroleum Geologists Bulletin*, 41, 1952–1984.
- Patterson, M. A., Sarson, G. R., Sarson, H. C., & Shukurov, A. (2010). Modelling the Neolithic transition in a heterogeneous environment. *Journal of Archaeological Science*, 37(11), 2929–2937.
- Perry, C. A., & Hsu, K. J. (2000). Geophysical, archaeological, and historical evidence support a solar-output model for climate change. *Proceedings of the National Academy of Sciences*, 97, 12433–12438.
- Playter, T., Corlett, H., Konhauser, K., Robbins, L., Rohais, S., Crombez, V., & Zonneveld, J. (2018). Clinoform identification and correlation in fine-grained sediments: A case study using the Triassic Montney formation. *Sedimentology*, 65, 263–302.
- Possehl, G. L. (2002). *The Indus civilization: A contemporary perspective* (p. 288). Rowman AltaMira.
- Rajesh, H. M., & Santosh, M. (2012). Charnockites and charnockites. *Geoscience Frontiers*, 3, 737–744.
- Ramkumar, M. (2001). Sedimentary microenvironments of modern Godavari delta: Characterization and statistical discrimination—Towards computer assisted environment recognition scheme. *Journal of the Geological Society of India*, 57, 49–63.
- Ramkumar, M. (2007). Spatio-temporal variations of sediment texture and their influence on organic carbon distribution in the Krishna estuary. *Indian Journal of Geochemistry*, 22, 143–154.
- Ramkumar, M. (2009). Flooding - a manageable geohazard. In M. Ramkumar (Ed.), *Geological hazards: Causes, consequences and methods of containment* (pp. 177–190). New India Publishers.
- Ramkumar, M. (2015). Discrimination of tectonic dynamism, quiescence, and third order relative sea level cycles of the Cauvery Basin, South India. *Geoloski Anali Balkanskoga Poluostrva*, 76, 19–45.
- Ramkumar, M., Balasubramani, K., Kumaraswamy, K., Santosh, M., Roy, P. D., Manobalaji, A., Juni, K. J., Nagarajan, R., Sharma, R., Kumar, P., Chopra, S., Siddiqui, N. A., Ramachandran, C., & Leo George, S. (2022). Episodic habitation and abandonment of Neolithic civilization sites in the Vaigai River basin, Southern India. *Geosystems and Geoenvironment*, 1, 100007.
- Ramkumar, M., & Berner, Z. (2015). Temporal trends of geochemistry, relative sea level and source area weathering in the Barremian-Danian strata of the Cauvery Basin, South India. In M. Ramkumar (Ed.), *Chemotatigraphy: Concepts, techniques and applications* (Vol. 631, pp. 273–308). Elsevier. <https://doi.org/10.1016/B978-0-12-419968-2.00011-X>
- Ramkumar, M., Kumaraswamy, K., Arthur James, R., Suresh, M., Sugantha, T., Jayaraj, L., Mathiyalagan, S. M., & Shyamala, J. (2015). Sand mining, channel bar dynamics and sediment textural properties of the Kaveri River, South India: Implications on flooding hazard and sustainability of the natural fluvial system. In M. Ramkumar, K. Kumaraswamy, & R. Mohanraj (Eds.), *Environmental management of river basin ecosystems* (pp. 283–318). Springer-Verlag. <https://doi.org/10.1007/978-3-319-13425-3-14>
- Ramkumar, M., Kumaraswamy, K., Balasubramani, K., Abdul Rahaman, S., Jegankumar, R., Kumara Ganesh, U., Manikandan, E., Balasundareswaran, A., Prithiviraj, G., Ayyanthurai, R., Santosh, M., Nagarajan, R., Siddiqui, N. A., Menier, D., Mathew, M. J., Ramachandran, C., Sathyaseelan, M., & Sivakumar, P. (2018). Discovery of buried historical structures through integrated geological and geophysical techniques in the Kaveri-Kollidam interfluvium, India: Implications for morpho-tectonics and archeological exploration. *Archaeological Prospection*, 26, 58–73.
- Ramkumar, M., Kumaraswamy, K., Balasubramani, K., Nagarajan, R., Santosh, M., Abdul Rahman, S., Arun Prasad, K., Juni, K. J., Fathima, A. L., Siddiqui, N. A., Mathew, M. J., Menier, D., Sautter, B., Rajveer, S., Pankaj, K., Sundeeep, C., & Jegankumar, R. (2021). Neolithic cultural sites and extreme climate related channel avulsion: Evidence from the Vaigai River basin, southern India. *Journal of Archaeological Science Report*, 40, 103–204. <https://doi.org/10.1016/j.jasrep.2021.103204>
- Ramkumar, M., Menier, D., Mathew, M. J., & Santosh, M. (2016). Geological, geophysical and inherited tectonic imprints on the climate and contrasting coastal geomorphology of the Indian peninsula. *Gondwana Research*, 36, 52–80.
- Ramkumar, M., Rani, P. S., Gandhi, M. S., Ramayya, M. P., Kumari, V. R., Bhagavan, K. V. S., & Swamy, A. S. R. (2000). Textural characteristics and depositional sedimentary environments of the modern Godavari Delta. *Journal of the Geological Society of India*, 56, 471–487.
- Ramkumar, M., Santosh, M., Abdul Rahaman, S., Balasundareswaran, A., Balasubramani, K., Mathew, M. J., Sautter, B., Siddiqui, S. N., Usha, K., Sreerhishya, K., Prithiviraj, G., Nagarajan, R., Thirukumaran, V., Menier, D., & Kumaraswamy, K. (2019). Tectono-morphological evolution of the Cauvery, Vaigai and Thamirabarani River basins: Implications on timing, stratigraphic markers, relative roles of intrinsic and extrinsic factors and transience of southern Indian landscape. *Geological Journal*, 54, 2870–2911.
- Rashid, H., England, E., Thompson, L., & Polyak, L. (2011). Late glacial to Holocene Indian summer monsoon variability based upon sediment. *Terrestrial, Atmospheric, and Oceanic Sciences*, 22, 215–228.

- Rashid, H., Flower, B. P., Poore, R. Z., & Quinn, T. M. (2007). A ~25 ka Indian Ocean monsoon variability record from the Andaman Sea. *Quaternary Science Reviews*, 26, 2586–2597.
- Rawat, V., Rawat, S., Srivastava, P., Negi, P., Prakasam, M., & Kotlia, B. S. (2021). Middle Holocene Indian summer monsoon variability and its impact on cultural changes in the Indian subcontinent. *Quaternary Science Reviews*, 255, 106825.
- Redman, C. L., James, S. R., Fish, P. R., & Rogers, J. D. (Eds.). (2004). *The impact of humans on their environment: The archaeology of global change* (p. 240). Smithsonian Books.
- Ristvet, L., & Weiss, H. (2005). The Habur region in the late third and early second millennium B.C. In W. Orthmann (Ed.), *The history and archaeology of Syria* (Vol. 1, pp. 1–26). Saarbrücken Verlag.
- Roser, B. P., & Korsch, R. J. (1988). Provenance signatures of sandstone-mudstone suites determine using discrimination function analysis of major-element data. *Chemical Geology*, 67, 119–139.
- Roy, D. K., & Roser, B. P. (2013). Geochemical evolution of the tertiary succession of the NW shelf, Bengal basin, Bangladesh: Implications for provenance, paleoweathering and Himalayan erosion. *Journal of Asian Earth Sciences*, 78, 248–262.
- Sajeev, K., Santosh, M., & Kim, H. S. (2006). Partial melting and P-T evolution of the Kodaikanal Metapelite Belt, southern India. *Lithos*, 92, 465–483.
- Santosh, M., Maruyama, S., & Sato, K. (2009). Anatomy of a Cambrian suture in Gondwana: Pacific-type orogeny in the southern India? *Gondwana Research*, 16, 321–341.
- Santosh, M., Yang, Q. Y., Shaji, E., Ram Mohan, M., Tsunogae, T., & Satyanarayanan, M. (2017). Oldest rocks from peninsular India: Evidence for Hadean to Neoproterozoic crustal evolution. *Gondwana Research*, 29, 105–135.
- Sharma, R., Umapathy, G. R., Kumar, P., Ojha, S., Gargari, S., Joshi, R., Chopra, S., & Kanjilal, D. (2019). AMS and upcoming geochronology facility at inter university accelerator Centre (IUAC), New Delhi, India. *Nuclear Instruments and Methods in Physics Research Section B: Beam Interactions with Materials and Atoms*, 438, 124–130.
- Singh, A., Thomsen, K. J., Sinha, R., Buylaert, J. P., Carter, A., Mark, D. F., Mason, P. J., Densmore, A. L., Murray, A., Jain, M., Paul, D., & Gupta, S. (2017). Counter-intuitive influence of Himalayan river morphodynamics on Indus civilization urban settlements. *Nature Communications*, 8, 1–14.
- Slater, L. J., & Singer, M. B. (2013). Imprint of climate and climate change in alluvial riverbeds: Continental United States, 1950–2011. *Geology*, 41, 595–598.
- Smith, J. T., & Comans, R. N. J. (1996). Modelling the diffusive transport and remobilisation of 137Cs in sediments: The effects of sorption kinetics and reversibility. *Geochimica et Cosmochimica Acta*, 60(6), 995–1004.
- Soubry, B., Sherren, K., & Thornton, T. F. (2020). Are we taking farmers seriously? A review of the literature on farmer perceptions and climate change, 2007–2018. *Journal of Rural Studies*, 74, 210–222. <https://doi.org/10.1016/j.jrurstud.2019.09.005>
- Sridhar, A. (2007). A mid-late Holocene flood record from the alluvial reach of the Mahiriver, Western India. *Catena*, 70, 330–339.
- Stanley, J. D., Krom, M. D., Cliff, R. A., & Woodward, J. (2003). Short contribution Nile failure at the end of the old kingdom, Egypt: Strontium isotopic and petrologic evidence. *Geoarchaeology*, 18, 395–402.
- Staubwasser, M., Sirocko, F., Grootes, P. M., & Segl, M. (2003). Climate change at the 4.2 ka BP termination of the Indus valley civilization and Holocene south Asian monsoon variability. *Geophysical Research Letters*, 30, 1425.
- Staubwasser, M., & Weiss, H. (2006). Holocene climate and cultural evolution in late prehistoric–early historic West Asia. *Quaternary Research*, 66, 372–387.
- Stewart, H. B. (1958). Sedimentary reflections on depositional environment in San Migne lagoon, Baja California, Mexico. *American Association of Petroleum Geologists Bulletin*, 42, 2567–2618.
- Stuiver, M., & Polach, H. A. (1977). Discussion: Reporting of C data. *Radio-carbon*, 19, 355–363.
- Sun, Y., Geo, S., & Li, J. (2003). Preliminary analysis of grain-size populations with environmentally sensitive terrigenous compounds in marginal sea setting. *Chinese Science Bulletin*, 48, 184–187.
- Suttner, L. J., & Dutta, P. K. (1986). Alluvial sandstone composition and paleoclimate; I, Framework mineralogy. *Journal of Sedimentary Research*, 56(3), 329–345.
- Thakur, S., Chudasama, B., Porwal, A., González-Álvarez, I. (2016). Sub-surface paleochannel detection in DeGrussa area, Western Australia, using thermal infrared remote sensing. In: Khanbilvardi, R., Ganju, A., Rajawat, A.S., Chen, J.M. (Eds.), *Land Surface and Cryosphere Remote Sensing III*, 9877, 294–306. <https://doi.org/10.1117/12.2223626>.
- Velde, B. (1995). Composition and mineralogy of clay minerals. In B. Velde (Ed.), *Origin and mineralogy of clays*. Springer. https://doi.org/10.1007/978-3-662-12648-6_2
- Verma, S. P., & Armstrong-Altrin, J. S. (2016). Geochemical discrimination of siliciclastic sediments from active and passive margin settings. *Sedimentary Geology*, 332, 1–12.
- Wang, J., Sun, L., Chen, L., Xu, L., Wang, Y., & Wang, X. (2016). The abrupt climate change near 4,400 yr BP on the cultural transition in Yuchisi, China and its global linkage. *Scientific Reports*, 6(1), 27723.
- Weiss, H. (2000). Beyond the younger Dryas—Collapse as adaptation to abrupt climatic change in ancient West Asia and the eastern Mediterranean. In G. Bawden & R. Keycraft (Eds.), *Confronting natural disaster: Engaging the past to understand the future* (pp. 75–98). University of New Mexico Press.
- Weiss, H., Courty, M. A., Wetterstrom, W., Guichard, F., Senior, L., Meadow, R., & Curnow, A. (1993). The genesis and collapse of third millennium north Mesopotamian civilization. *Science*, 261, 995–1004.
- Weninger, B., Alram-Stern, E., Bauer, E., Clare, L., Danzeglocke, U., Joris, O., Kubatzki, L., Rollefson, C., Todorova, H., & van Andel, T. (2006). Climate forcing due to the 8200 cal BP event observed at early Neolithic sites in the eastern Mediterranean. *Quaternary Research*, 66, 401–420.
- Wulf, H., Bookhagen, B., & Scherler, D. (2010). Seasonal precipitation gradients and their impact on fluvial sediment flux in the northwest Himalaya. *Geomorphology*, 118, 13–21.
- Xie, G., Shenc, Y., Liuab, S., & Haod, W. (2018). Trace and rare earth element (REE) characteristics of mudstones from Eocene Pinghu formation and Oligocene Huagang formation in Xihu sag, East China Sea basin: Implications for provenance, depositional conditions and paleoclimate. *Marine and Petroleum Geology*, 92, 20–36.
- Zhao, K., Wang, Y., Edwards, R. L., Cheng, H., Liu, D., & Kong, X. (2015). A high-resolution record of the Asian summer monsoon from Donggucave, China for the past 1200 years. *Quaternary Science Reviews*, 122, 250–257.

SUPPORTING INFORMATION

Additional supporting information can be found online in the Supporting Information section at the end of this article.

How to cite this article: Ramkumar, M., Nagarajan, R., Juni, K. J., Manobalaji, A., Balasubramani, K., Roy, P. D., Kumaraswamy, K., Fathima, A. L., Pramod, A., Sharveen, R., Rahman, S. A., Siddiqui, N. A., Menier, D., & Sharma, R. (2024). Tectono-climatic and depositional environmental controls on the Neolithic habitation sites, Vaigai River Basin, Southern India. *Geological Journal*, 1–20. <https://doi.org/10.1002/gj.4919>